

Politecnico di Torino / CEA Grenoble

Master's Degree Course in Mechanical Engineering



**Politecnico
di Torino**

Master's Degree Thesis

Integration of Distributed Storages In District Heating Networks For Supply Temperature Reduction

Internship Tutors:

Nicolas LAMAISON

Nicolas VASSET

Candidate:

Alessia PATERNOSTRO

University Tutor:

Elisa GUELPA

2022-2023

Abstract

District heating networks (DHN) are an essential component of a low-carbon ecosystem for energy in the residential sector. In particular, they enable efficient heat supply in urban areas, with very low CO₂ emissions. In order to improve the efficiency of these networks and to be able to integrate low carbon production assets (heat pumps, solar thermal...), an effort has to be made for lowering the network operation temperature levels. This kind of transformation often requires intervention on the network design in order to upgrade part of the existing installation (pipes, substations, pumps). The integration of thermal storage solutions, strategically located on the distribution network and adequately piloted, is particularly promising. This research focuses on the utilization of sensible heat water tanks as a thermal storage solution and seeks to assess the extent to which they can contribute to the adaptability of real-world district heating networks. The aim of the present work is to analyze the behavior of the storage integrated in a DHN and to demonstrate the benefits that a distributed storage can bring. With the objective of studying the operation of the network with and without storage, a one-dimensional model of the storage has been applied to a real case-study. More specifically, a set of distributed heat storages has been integrated into a detailed model of the district heating network of the city of Metz (France), with the aim of uncoupling demand from supply. As DH network evolves toward lower temperatures, the design of such systems is more complex, and it is crucial to maintain a high thermal and economic performance. Several simulations were performed to obtain an optimal design of the network at different temperature levels, considering an economic perspective.

Acknowledgements

I would like to express my heartfelt gratitude to the following individuals and organizations for their invaluable support and contributions throughout the course of my research and the completion of this thesis at the CEA's Liten Institute (CEA is a technological research institute specializing in energy transition technology in the French State).

My Supervisors at CEA, Nicolas Lamaison and Nicolas Vasset

I am deeply indebted to Nicolas Lamaison and Nicolas Vasset for their unwavering guidance, mentorship, and expertise. Their insights and feedback have been instrumental in shaping the direction of my research and the quality of this thesis.

My Supervisor at Politecnico di Torino, Elisa Guelpa

I extend my appreciation to Prof. Elisa Guelpa, for her valuable input and constructive critique, which greatly enriched the content of this thesis.

My Colleagues and Labmates

I would like to acknowledge the collaborative spirit and camaraderie among fellow researchers in the Energy Systems Laboratory for the Territories (LSET) at the CEA. Their support, monthly meetings, and shared resources have been pivotal in the success of my research.

Family and Friends

My deepest gratitude goes to my family for their unwavering support, and to my friends for their encouragement and understanding as I pursued this research endeavor.

The Vision of CEA

The CEA's Liten Institute has provided an inspiring and collaborative environment that fosters groundbreaking research. I am proud to have been part of this institution.

Additional Contributions

To all those who played a part in the successful completion of this research, whether mentioned here or not, I extend my sincere appreciation.

My journey at the CEA has been a remarkable and rewarding experience, and I am profoundly thankful to everyone who has contributed to this thesis.

Alessia Paternostro

CEA's Liten Institute

19/10/2023

INDEX

List of figures	8
Acronyms	10
Nomenclature	11
1. Introduction	12
1.1 Case-Study	14
1.2 Tools.....	14
2. An overview of District Heating Networks.....	15
2.1 Generations of District Heating Systems	15
2.2 Towards the decarbonization	17
2.2.1 Advantages of Lowering the Supply Temperature in District Heating.....	17
2.2.2 Constraints in supply temperature reduction.....	19
3. Thermal Energy Storage.....	22
3.1 TES as a source of flexibility	22
3.2 Distributed thermal energy storage.....	23
3.3 Design parameters and operational principles of a TES	24
3.4 Storage tank model.....	26
3.4.1 Model in DistrictLab-H	26
3.5 Simulation of TES	27
4. Case study Setup.....	29
4.1 Network description	29
4.2 Methodology to identify the bottlenecks	30
4.3 TES integrated in the case-study.....	33
4.3.1 Favorable position and sizing.....	35
4.3.2 Not Favorable position and sizing.....	36
4.3.3 Impact of the piloting of the charging phase on the discharging phase	40
5. The Optimization Process	43
5.1 Characteristics of the Optimization	43
5.1.1 Multi-objective optimization	43
5.1.2 Genetic algorithm	44
5.2 Optimization method for Storage Location and Size Selection	45
5.3 Integration of storages in the optimization process.....	46
5.3.1 Decision space	46
5.3.2 Objective functions.....	48

6. Results.....	50
6.1 Unitary test	50
6.2 Detailed results for a supply temperature of 115 [°C].....	52
6.2.1 Details on the proposed solution.....	54
6.3 Effect of the supply temperature on the results	55
6.4 Discussion regarding initial conditions of the storage.....	59
7. Conclusion and Perspective	62
Bibliography.....	64

List of figures

Figure 1. Annual global energy supplies to district heating networks in the Net Zero Scenario, 2010-2030. [2].....	14
- Figure 2. Benefits achieved by the reduction of the supply temperature in existing DH. [6].....	18
Figure 3. Dependency of water velocity and pressure along the pipes on the supply T. [6].....	20
Figure 4.Example of variable heat demand of a substation	22
Figure 5. Distributed thermal storages in a DHN.....	23
Figure 6.Directly connected storage and pressure-separated storage. [14]	25
Figure 7. Schematic representation of a heat storage model.....	27
Figure 8.Temperature distribution of six sections of the storage; mass flow rate during charging/discharging phase.....	28
Figure 9. DH subnetwork of the city of Metz.....	29
Figure 10. Above: Heat demand profile and the transferred heat. Below: External temperature profile.	30
Figure 11. Linear pressure losses.....	31
Figure 12. Velocity along the pipes.....	32
Figure 13. Minimum differential pressure at each substation	32
Figure 14.Critical temperature	33
Figure 15. Five TESs integrated in the DHN of Metz	34
Figure 16. Configuration of the network for the simulation “Favorable position and sizing”	35
Figure 17.Profile of the velocity [m/s] in the most critical pipe; Mass flow rate [kg/s] inside the storage.	36
Figure 18. Configuration of the network for the simulation “Not Favorable position and sizing”.	37
Figure 19. Profile of the velocity [m/s] in the most critical pipe; Mass flow rate [kg/s] inside the storage; SST 5 Heat Demand-Heat Transferred [W].	38
Figure 20. Comparison between critical temperature [°C] of a SST and fluid mean temperature [°C] of the pipe upstream the SST.....	38
Figure 21. New simulation: Profile of the velocity [m/s] in the most critical pipe; Mass flow rate [kg/s] inside the storage; Heat Demand-Heat Transferred [W].....	39
Figure 22. Comparison between critical temperature [°C] of a SST and fluid mean temperature [°C] of the pipe upstream the SST.....	40
Figure 23. Temperature [°C] profile of six layers of STORAGE_5 in the scenario 1.	41
Figure 24. Temperature [°C] profile of six layers of STORAGE_5 in the scenario 2.	41
Figure 25. Average temperature of the first 10 top layers of the storage during the discharging time.	42
Figure 26. Combination of optimization algorithm (on the left) and dynamic simulator (on the right).	45
Figure 27. Network with the highlighted elements populating the decision space of the optimization framework.	48
Figure 28. District heating network including five storages.	50
Figure 29. Pareto front of the case study 5 at 115 [°C].....	52
Figure 30. Comparison of the Pareto Curve in two scenarios: with and without storages.	53
Figure 31. Location of the detailed assets.	54
Figure 32. Pareto front at 115 [°C] with details on the STORAGE_5.....	54
Figure 33. Pareto front at 115 [°C] with details on the PUMP_4 in the scenario with storages.....	54
Figure 34. Pareto front at 115 [°C] with details on the PUMP_4 in the scenario without storages.	55

Figure 35. Comparison of the Pareto Curve in two scenarios: with and without storages at four different temperature levels. 55

Figure 36. Pareto front at different temperature with details on the SST1 (on the top part) and SST5 (on the bottom part)..... 57

Figure 37. Pareto front at different temperature with details on the STORAGE_1 (on the top part) and STORAGE_5 (on the bottom part). 58

Figure 38. Configuration of the network with the highlighted assets. 59

Figure 39. Scenario 1: temperature [°C] distribution inside the storage..... 60

Figure 40. Scenario 2: temperature [°C] distribution inside the storage..... 60

Acronyms

2GDH	Second-generation district heating
CEA	Alternative Energies and Atomic Energy Commission
DEAP	Distributed Evolutionary Algorithms in Python
DH	District heating
DHN	District heating network
DHS	District heating system
GA	Genetic algorithm
MINLP	Mixed Integer Non-Linear Programming
MOO	Multi-objective optimization
NZE	Net Zero Emissions
RES	Renewable energy sources
SST	Substation
TES	Thermal energy storage

Nomenclature

η	Second law efficiency
T_b	Temperature of the building
T_s	Temperature of the source
T_0	Ambient temperature
Q_{TES}	Energy storage capacity
ρ	Density of the heat transfer fluid
c_p	Specific heat of liquid water
V_{TES}	Storage volume
\dot{m}	Mass flow rate
ΔT	Difference in temperature
$t_{ch,disch}$	Time of the charging or of the discharging phase
$Q_{ch,disch}$	Desired energy content reached during the charging/discharging phase

1. Introduction

In a world marked by geopolitical instability and environmental imperatives, this thesis addresses a crucial global challenge. It operates within the context of a compelling need to transition away from fossil fuels, especially in the domain of district heating, and to advance the integration of renewable energy sources. Heating, cooling, and domestic hot water represent a significant portion of global building energy consumption, necessitating an imperative shift towards renewable thermal solutions.

District heating networks (DHN) play a vital role in this transition towards a low-carbon ecosystem for energy in the residential sector. They enable efficient heat supply in urban areas with remarkably low CO₂ emissions. However, to fully optimize these networks and integrate low-carbon energy production assets such as heat pumps and solar thermal systems, substantial efforts are needed to lower the operational temperature levels of these networks. This transformation often involves interventions in network design and infrastructure upgrades, including pipes, substations, and pumps. Moreover, strategically incorporating thermal storage solutions emerges as a promising avenue for enhancing district heating networks' adaptability and sustainability.

This thesis, therefore, navigates the intricate domain of sustainable district heating, with a specific focus on the transformative potential of Thermal Energy Storage (TES) as a retrofit solution. Its central aim is to evaluate the invaluable contributions that thermal energy storage systems can make to the retrofitting of existing district heating networks, thus moving us closer to a greener and more economically viable future. In achieving this goal, the work is structured into distinct chapters, each with a unique role and objective:

- Chapter 2: Context and Overview

In this initial chapter, it is provided a comprehensive context for the thesis, outlining the pressing need for sustainable district heating solutions. It delves into the different generations of district heating systems, from their steam-based origins in the late 1800s to the modern concept of ultra-low temperature district heating, it represents an impressive journey of innovation and sustainability. The central strategy of reducing supply temperatures emerges as a cornerstone in the quest for decarbonization, offering an array of benefits, including enhanced energy efficiency and the integration of renewable energy sources. However, this transition is not without its complexities, possible limitations are presented in this chapter. Despite these challenges, the overarching goal is clear: to propel district heating systems into a greener and more efficient future.

- Chapter 3: Modeling and Simulation

It serves as a foundational exploration of the numerical modeling and simulation aspects of the research. It introduces a finite difference numerical model of a stratified tank, a key component in the district heating network. The model relies on the use of linear systems that, once solved, will give the temperature of water at some points along the vertical axis of a large reservoir. This model is a fundamental building block for the subsequent analyses and simulations.

- Chapter 4: The Case-Study

Chapter 4 of this work presents a case study in which the behavior of distributed thermal energy storage (TES) in a district heating network (DHN) is examined. The study is conducted in the context of the Metz DH network in France, focusing on retrofitting a second-generation DHN to lower its temperature. The chapter provides a network description, including its components and operational conditions. It outlines a methodology for identifying network

bottlenecks based on various criteria. The integration of TES into the case study is discussed, along with the selection of storage locations and sizes to meet network constraints. The chapter also explores the impact of different charging and discharging strategies on TES performance. It concludes by emphasizing the importance of understanding the dynamic relationship between charging and discharging phases in TES systems for effective design and optimization.

- Chapter 5: Enhancing Flexibility and Optimization

Chapter 5 focuses on the optimization process in the context of energy-efficient heating systems and district heating networks. It introduces multi-objective optimization and Genetic Algorithms as key tools for solving complex problems. The chapter discusses the decision variables for optimization, including pipes, substations, booster pumps, and thermal energy storage. It also covers the evaluation of solutions based on capital and operational expenditures.

- Chapter 6: Results

In the penultimate chapter, the results of applying the optimization method to different test cases in a DHN are presented. The focus is on validating the inclusion of energy storage assets in the optimization process. The chapter discusses unitary tests that involve different storage configurations and their impact on the network. It also explores detailed solutions for a fixed supply temperature and examines how the results vary with changes in supply temperature.

- Chapter 7: Concluding Insights and Future Directions

The final chapter synthesizes the findings of our research and offers insights into the vital role of TES in district heating networks, particularly in the context of lowering operating temperatures. It is reflected on the practical implications of the work and suggest potential avenues for future research and practical application.

This thesis endeavors to contribute to the body of knowledge surrounding sustainable district heating, highlighting the pivotal role of TES in the transition to a more eco-friendly and energy-efficient future.

1.1 Sustainable District Heating: The TES Retrofit Solution

The utilization of fossil fuels is facing growing controversy due to various reasons, including geopolitical instability, environmental consequences such as climate change and air pollution. Consequently, there is a growing emphasis on the adoption of alternative renewable energy sources. In the realm of electricity generation, hydropower, photovoltaics, and wind turbines play significant roles in addressing these concerns. However, the situation is less established when it comes to the heating and cooling sector. Space heating, cooling, and domestic hot water together account for approximately half of global energy consumption in buildings [1]. This underscores the importance of pursuing renewable solutions for the thermal sector as well. District heating (DH) emerges as a key component of low-carbon heat strategies, particularly in countries like the Netherlands and the United Kingdom, as well as in cities like Paris, Munich, and Vancouver. Renewables represented just about 5% of district heat supplies globally, although this share can be over ten times higher in some countries. While bioenergy and renewable municipal waste account for the large majority of renewable district network supplies, large-scale solar thermal systems, geothermal energy and heat pumps are seeing growing interest (Figure 1). Europe currently leads renewables integration in district heating, with around 25% of its district heat supplies produced from renewable sources. In the NZE (Net Zero Emissions) Scenario, district heating continues to supply a similar share of global final heat consumption, although energy efficiency improvements in district heating networks and in building envelopes allow for a decline in district heat supplies by 2030, down by more than 15% compared with 2022. In the same period, renewable energy used in district networks more than doubles from current levels, with renewable

sources (including renewable electricity used by large-scale heat pumps) representing almost one-fifth of district heating supplies by 2030 [2].

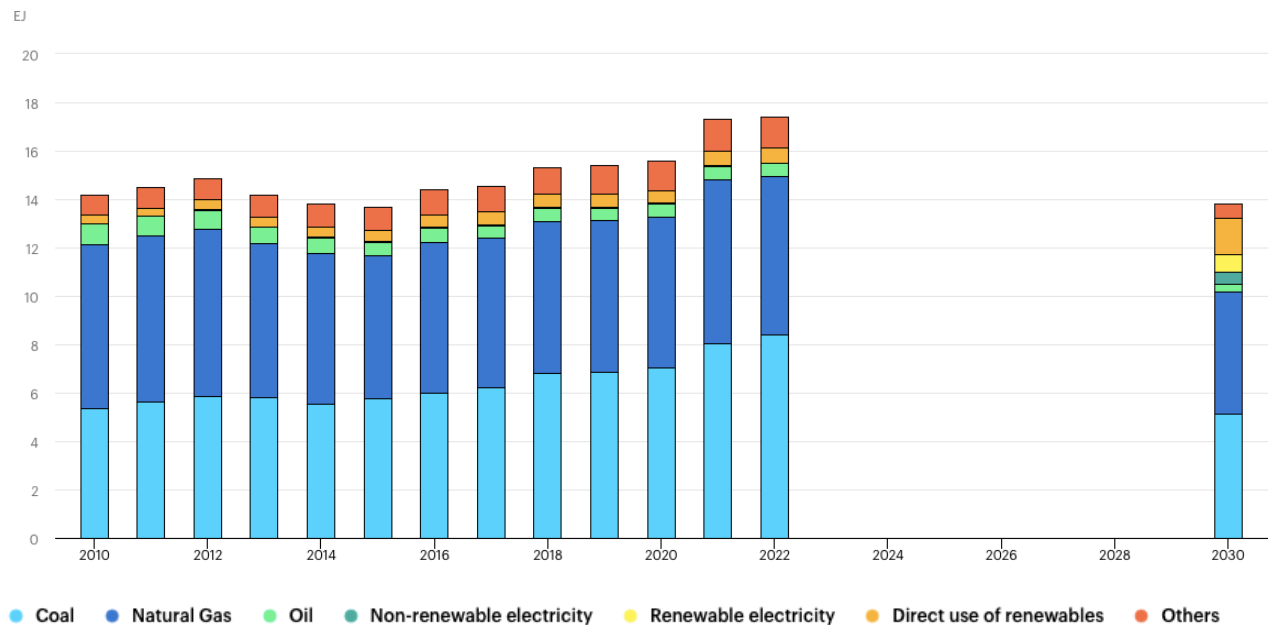


Figure 1. Annual global energy supplies to district heating networks in the Net Zero Scenario, 2010-2030. [2]

In this thesis, it is first provided an overview of the current state of district heating technology and its probable future developments. As it is elucidated, fossil fuels continue to dominate energy production in both district and individual heating. Therefore, it remains imperative, at least in the foreseeable future, to evaluate flexibility solutions in the context of increased efficiency and more rational use of renewable energy sources. Subsequently, flexibility solutions are briefly presented, ultimately leading to the consideration of Thermal Energy Storage (TES) with the aim of integrating RES.

1.2 Case-Study

The aim of the present work is to analyze the behavior of a storage integrated in a DHN and to demonstrate the benefits that a distributed TES can bring to a DHN, in the context of studying retrofitting solutions of existing 2DHN to achieve the goal of lowering the temperature. The present work has been applied to the real-life context of a DH network in the city of Metz (France).

1.3 Tools

A thermal hydraulic simulator has been used to describe dynamical operation of the DHN under study, and assess the current system potential, as well as the evaluation of design choices based on detailed scenarios. The software is DistrictLab-H [3], designed and developed by CEA team in Grenoble and Le Bourget du Lac (INES). It features a fast solver designed for the resolution of large scale and complex DH simulation problems relying on multi-threading and optimized memory management. The resolution strategy is based on the strong coupling between a quasi-steady state hydraulic problem, i.e., the solving of the pressure and velocity fields, and a pure dynamical thermal problem, i.e., the derivation of the temperature transportation through the network. This framework, although designed for dynamical calculations can support both static and dynamic simulations. For what concerns the optimization process, an already existing methodology for multi-objective design optimization has been exploited, using the thermal hydraulic simulator as evaluation function. This framework was implemented in Python 3.9 thanks to the use of the library DEAP [4].

2. An overview of District Heating Networks

District heating networks distribute thermal energy, typically in the form of hot water (or steam for historical networks), from a central source to residential, commercial, and industrial consumers. This energy is used for space heating, domestic hot water heating, process heating, cooking (when steam is used), and humidification. DH systems offer significant advantages by enhancing the efficient use of energy resources and facilitating the integration of renewable energy sources (e.g., geothermal heat, solar heat, biomass combustion heat) and surplus heat (e.g., industrial waste heat, waste incineration) into the heating sector.

2.1 Generations of District Heating Systems

District heating has evolved through several distinct generations, each characterized by unique thermodynamic parameters, materials, and heat sources. These generational shifts have aimed to improve efficiency, safety, and environmental considerations. Here is an overview of the different generations of district heating:

- First Generation (Late 1800s):

The initial generation of district heating (DH) systems can be traced back to the era of the Second Industrial Revolution during the late 1800s. In this period, urban areas primarily relied on individual building-based boilers to provide heat. These boilers, often fueled by solid coal, operated at high pressures and were responsible for heating water or generating steam. However, they presented several challenges: manual operation, complex maintenance, heat losses, safety risks (high operating pressures posed safety risks, including the potential for malfunction or even explosions) [5]. To simplify the heating process and improve the efficiency, a transition was made to larger central boilers. These boilers were connected to buildings through a network of pipes that transported high-pressure, high-temperature steam. The steam generated in the central boilers was then condensed in heat exchangers located within the buildings they served. While steam-based district heating systems were prevalent in northern Europe and North America during that time, only a few of them, such as those in Paris and New York City, remain operational in their original form today. It is worth noting that air pollution resulting from decentralized coal boilers was significant during this period, although environmental concerns were not a major focus at that time.

- Second Generation (Around 1930):

The second generation of district heating (DH) systems began to emerge around 1930. Prior to this period, it was recognized that hot water offered advantages over steam, but its effective use required the availability of electric pumps, which were becoming increasingly common at that time. The second-generation DH systems were characterized by several key features [6]:

- **Pressurized Hot Water Usage:** Hot water was chosen as the heat carrier, as it was considered a superior alternative to steam.
- **Electric Pumps:** The adoption of electric pumps facilitated the movement of hot water within the DH systems.
- **Pipe Configuration:** These systems featured smaller supply pipes, that were often installed within concrete ducts.
- **High Supply Temperatures:** Despite the shift to hot water, the supply temperatures remained relatively high, typically exceeding 100°C.

One notable aspect of the second-generation DH systems was the emphasis on not only centralizing heat production but also integrating the combined generation of electric power and heat (cogeneration). This integration aimed at conserving primary energy resources.

- Third Generation (Around 1970):

The onset of the third generation of district heating occurred in northern European countries around 1970 [5]. This phase was characterized by a shift towards using hot water with reduced operating temperature, aiming to stay below the 100 °C threshold. This transition had several important implications as the use of lighter and more cost-effective materials, including polymers, thanks to lower operating parameters, the integration of various heat sources, including the utilization of large heat pumps. The shift also simplified the installation of components, with a particular emphasis on the adoption of pre-insulated pipes. Reducing the thermal level of the delivered heat had clear physical benefits. It resulted in the increased generation of electric power when combined plants were employed, and it led to reduced thermal losses. This generation aimed to improve overall efficiency and sustainability in district heating systems.

- Fourth Generation (Ongoing):

The fourth generation of district heating (DH) systems is being developed as a response to the growing need for the integration of higher proportions of renewable energy sources into heating and for further reduction in energy losses. This generation represents an evolutionary step from the third generation, with a focus on several key aspects:

- Lighter Components: The fourth generation continues the trend of using lighter and more efficient components.
- Cost-Effective Materials: It emphasizes the use of cost-effective materials.
- Reduced Pressures and Temperatures: An essential feature is the reduction in operating pressures and temperatures, typically targeting around 1 bar and 70°C.

The fourth generation of DH systems is designed to enhance sustainability by incorporating more renewable energy sources, reducing losses, and optimizing energy efficiency.

- Fifth Generation (Since Around 2010):

In recent years, the development and implementation of fifth-generation district heating networks, which emerged around 2010, have introduced innovative concepts. These networks aim to achieve even lower network temperatures, approaching ambient levels within the range of 0-45°C. This specific temperature range is often referred to as "ultra-low temperature district heating" (ULTR-DH). ULTR-DH systems necessitate the use of heat pumps by customers to effectively extract and release heat. This approach enables a significant decentralization of heat and cold production within the district heating network. It also opens up new business models where consumers actively participate in both heat and cold production processes, transforming them into producers as well. In summary, fifth-generation district heating networks, with their ultra-low temperature approach and customer-involved heat pump technology, facilitate a higher degree of decentralization in heat and cold production while fostering innovative consumer-driven business models [7].

2.2 Towards the decarbonization

In 2022 district heat¹ production remained relatively similar to the previous year, meeting around 9% of the global final heating need in buildings and industry [8]. District heating networks offer great potential for efficient, cost-effective and flexible large-scale integration of low-carbon energy sources into the heating energy mix. However, the decarbonization potential of district heating is largely untapped, as fossil fuels still dominate district network supplies globally (about 90% of total heat production), especially in the two largest markets of China and Russia. Aligning with the Net Zero Emissions by 2050 Scenario requires significant efforts to rapidly improve the energy efficiency of existing networks, switch them to renewable heat sources (such as bioenergy, solar thermal, heat pumps and geothermal), integrate secondary heat sources (such as waste heat from industrial installations and data centers), and to develop high-efficiency infrastructure in areas with dense heat demand. [8]

As it is described in the section 2.1, district heating (DH) were mainly based on high temperature heat carriers and divided into different generations: 1st generation DH fed by steam ($T \gg 100$ [°C]), 2nd generation DH fed by pressurized overheated water ($T > 100$ [°C]), 3rd generation DH, fed by hot water ($T < 100$ [°C]). Nowadays the tendency is to design DH systems to operate with low and ultra-low temperature heat carriers and even temperatures close to the ambient (neutral temperatures). Low temperature DHs operate between 50 and 70 [°C]; ultra-low temperature DHs operate between 35 and 50 [°C]; neutral DHs operate at a temperature of about 20–35 [°C] [6]. Many of the current operational district heating systems fall within the second and third generations, functioning with supply temperatures exceeding 80–100 [°C]. To align with long-term decarbonization goals, it is imperative to transition these existing networks into low-temperature systems in a manner that is both economically viable and efficient.

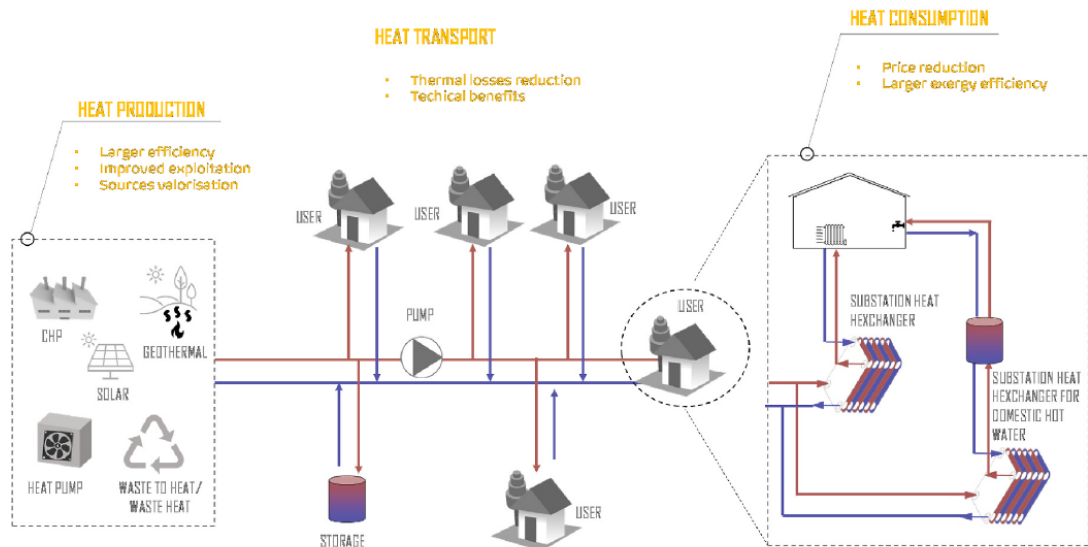
The unequivocal significance of adopting low-temperature heat carriers in district heating lies in its capacity to accomplish several critical objectives:

- exploit renewable energy (often available at lower temperature);
- valorize industrial waste heat (available at lower temperature);
- reduce thermal losses;
- increase the efficiency of the technologies used for heat production (e.g. combined heat and power plants and heat pumps) and use low-cost technologies (i.e. plastic pipes for distribution).

2.2.1 Advantages of Lowering the Supply Temperature in District Heating

In the literature, the benefits that can be achieved by reducing the supply temperature in the DHS are analyzed, the authors of [6] presented a classification of benefits (Figure 2) according to the various sections of the system:

- Heat production side;
- Heat transport side;
- Heat consumption side.



- Figure 2. Benefits achieved by the reduction of the supply temperature in existing DH. [6]

Heat production side

It is possible to use low-temperature sources as more industrial waste heat, solar energy, and geothermal heat can be integrated. Moreover, it enhances the second law efficiency of various heat generation technologies, including both conventional methods and renewable heat sources. This improvement stems from the fact that as the source temperature decreases (subscript 's'), the denominator in the Equation 1 below decreases. If the building requirement did not change in terms of temperature (T_b) then the system efficiency increases.

$$\eta = \frac{\phi_b \left(1 - \frac{T_0}{T_b}\right)}{\phi_s \left(1 - \frac{T_0}{T_s}\right)}$$

Equation 1

The effects of reducing supply temperatures vary depending on the technology used:

- *Steam-based Combined Heat and Power plants (CHP)* can optimize the power-to-heat ratio by expanding to lower pressure and temperature levels, resulting in increased electricity production and up to a 25% improvement in second law efficiency with a 30 [°C] supply temperature reduction.
- Heat production from *waste incineration* and *biomass fuels* can be augmented by directly condensing flue gases, leading to an expected 25% increase in recovered heat.
- *Heat pumps* benefit from lower condensation temperatures, significantly boosting their coefficient of performance (COP) and offering a 20–25% real COP increase when supply temperature is reduced from 100 [°C] to 70 [°C].
- Additional *geothermal heat* sources can be integrated, particularly with large geothermal resources available in Europe at temperature levels of 40–80 [°C], resulting in significant benefits.

- *Solar energy* can effectively supply low-temperature networks, as lower temperatures positively impact the efficiency of thermal collectors.

It is worth noting that while reducing supply temperatures can have negative effects on *Heat Only Boilers* due to corrosion and temperature gradient issues, the aim is primarily to exploit waste heat and renewable sources in district heating systems. Heat Only Boilers are not expected to play a major role in future energy systems.

Heat transport side

Lower operating temperatures in district heating systems result in reduced heat losses along the network. It has been estimated that, in conjunction with a well-designed network, low temperatures have the potential to decrease heat losses by as much as 75% compared to conventional designs [9]. Even in existing networks, reductions of up to 35% in heat losses are achievable. Low supply temperatures result in smaller temperature differentials between supply and return, which can either reduce the network capacity or necessitate increased mass-flow rates and, consequently, higher pressure drops along the network. However, real-world applications demonstrate that, while reducing the supply temperature saves a significant amount of heat, the increased energy required for pumping can be managed and limited [10]. Beyond the reduction in heat distribution losses, there are additional advantages:

- the ability to use cost-effective plastic pipes in low-pressure areas, which is more economical than traditional metal-based pipes, particularly for network extensions;
- a reduced risk of water boiling in the network;
- decreased thermal stress on pipes, leading to lower maintenance costs;
- a lower risk of pipe leaks with respect to the higher temperature;
- a reduced risk of scalding when performing pipe maintenance.

Additionally, thermal storage units, that operate in low-temperature systems, have the advantage of lower thermal losses. However, the storage capacity of sensible thermal storage units decreases as the temperature difference between supply and return decreases. Temperature reduction also enables the possibility of long-term storage, including seasonal storage, as storing water above boiling temperature becomes cost-prohibitive [10].

Heat consumption side

The reduction in temperature leads to reduce system energy losses and, from a consumer point of view, there is the possibility to reduce the prices, due to the improvement of the efficiency in the system.

In Western Europe, an important share of DH energy is still delivered relying on 2nd generation technologies [10]. The transition of existing 2GDH networks towards lower temperature levels for operation is needed and, in this context, retrofitting measures on the distribution network are required in order to guarantee the heat demand satisfaction. 2DGH systems are designed to operate with high temperature water, moreover DH is an infrastructure with high investment cost (due to the difficulties of pipe installation in the ground), these are limits in the process towards lower temperature.

2.2.2 Constraints in supply temperature reduction

Reducing the supply temperature in an existing DH network leads to some constraints that can be classified according to the part of the network that is involved [6]:

- Limitations at the network level
- Limitations at the substation level
- Limitations at the building level

Network level

When the supply temperature is decreased, the supply-return temperature difference is smaller, this causes an increase in the mass flow rate that circulate in the network and, consequently, an increase in pressure losses. One of the effects is the increase of energy for pumping, even if, compared with the reduction of heat losses, it is contained and limited. The other effect concerns the water velocity in the pipes: higher mass flow rate causes water congestion in the pipelines. This congestion occurs when a greater mass of water flows in pipelines designed for lower mass flow rates. Two main consequences arise:

- Increased Water Velocity: some sections of the network may experience high water velocities due to smaller pipe diameters designed for lower flow rates, potentially leading to mechanical vibrations and inadequate supply.
- Exceeding Maximum Pressure: higher mass flow rates to compensate for reduced supply temperature can lead to exceeding the maximum operating pressure of the network, which is a technical limitation.

The impact of supply temperature reduction on water flow velocity and pressure losses depends significantly on the temperature difference between the supply and return lines. These effects are nonlinear, with larger reductions in temperature difference resulting in more significant increases in velocity and pressure losses (Figure 3 that shows the dependency of the velocity and pressure losses on the temperature in a 1 m long network).

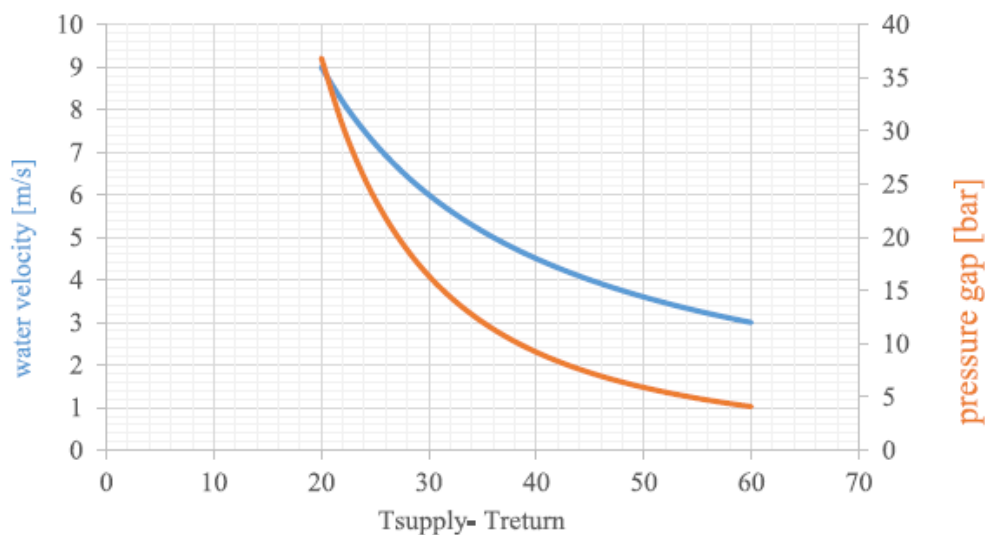


Figure 3. Dependency of water velocity and pressure along the pipes on the supply T. [6]

Substation level

The capacity of the substations to supply the energy requested is reduced by lowering the temperature. The main limits are:

- the critical temperature that corresponds to the primary inlet temperature limit under which the secondary thermal demand can no longer be satisfied, regardless of the selected mass flow rate;
- the maximum mass flow rate that can flow through the substation, associated to the hydraulic sizing.

Building level

The design of the radiators takes into account the most extreme climatic conditions in the specific region, typically ranging from -5°C to -15°C in European climates. Consequently, it is plausible to assume that, for most of the year, the typical space heating demands (excluding extremely cold days) can be met by using lower supply temperatures. Low temperature heat could limit the thermal power exchange in the heat devices (i.e. radiators designed to operate with supply temperature between 90°C and 70°C) [10].

3. Thermal Energy Storage

In the literature, many studies show different solutions to be applied in order to solve the limitations that arise when the supply temperature of the network is reduced [6], [11]. These limitations are called bottlenecks. They can be solved adopting different strategies as:

- Modifications of the network topology (adding new branches to create loops);
- Actions on the pumping system (possibility to add booster pumps);
- Substitutions of the bottleneck pipes with pipes with larger diameter;
- Installations of new devices to store the energy when the demand is low and to provide it when the demand is lower.

Thermal energy storage (TES) is largely used in district heating and cooling systems as a solution for solving some bottleneck-type issues. TES is by definition a device of containment that allows energy, traditionally water-based thermal energy, to be stored for future use, ideally with limited losses [12]. This is useful to reduce the heat at the central unit when the demand is highly variable during the day (see Figure 4).

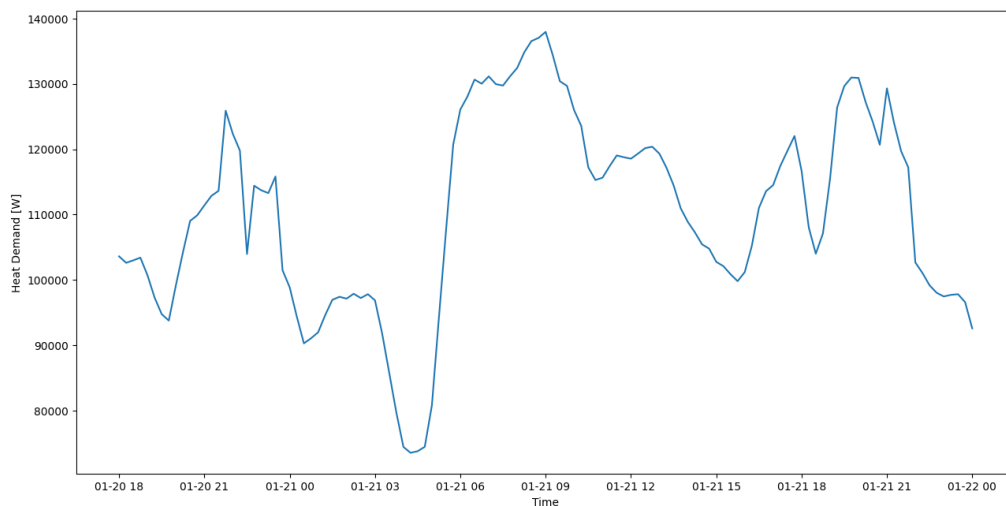


Figure 4. Example of variable heat demand of a substation

3.1 TES as a source of flexibility

The connection between the heat production cost in a DHN and the electricity market is influenced by the technology used in the heat production plant. In a DHN where cogeneration is used, the heat production plant generates both heat and electricity simultaneously. The connection with the electricity market occurs because any surplus electricity produced can be sold to the electricity grid, potentially affecting the overall cost structure. For example, when electricity prices are high, selling surplus electricity can offset some of the heat production costs, making heat production more economical. When heat pumps are employed in the DHN, they are powered by electricity. In this case, the cost of electricity from the electricity market directly influences the heat production cost. When electricity prices are high, the cost of running heat pumps can be elevated, affecting the overall cost of providing heat in the DHN. However, if the DHN relies on other forms of heat production that are not directly tied to electricity generation or consumption, then the connection to the electricity market

is less direct and may primarily involve the purchasing of electricity for the DHN's own operational needs.

Regarding the pricing structure in the electricity market, it has become volatile with the introduction of more wind, solar and hydropower. These energy sources are not flexible, and the energy production cannot be shifted in time; this energy should be either consumed instantaneously or wasted. Moreover, the heat demand of buildings is mostly driven by external temperature levels and so the demand profiles are fixed as well [13]. TES is installed in the DH network to handle the mismatch in between production (heat supply) and consumption (heat demand) and it is an effective solution to reduce the heat load variations, providing flexibility to the DH system. TES is behaving as a prosumer: it stores energy when the demand is low (end users behavior) and it provides energy when the demand is high (central plant behavior). The integration of storage capacity in a DH system allows the controller to source optimize, so that the cheapest production unit is fully utilized at all time when it is available. The most common sensible systems are based on liquid water, accumulated in tanks that range in size from hundreds of liters in households, to hundreds of cubic meters in tanks for daily and hourly balancing in DH networks, and up to hundreds of thousands of cubic meters in large reservoirs sometimes used for seasonal energy storage [14]. Let us remember that water has relatively high thermal conductivity and density, and the highest sensible heat capacity per unit of mass of all naturally occurring substances. It is liquid and therefore easy to move and to use as a heat transfer fluid as well, it has low viscosity, it is chemically inert, non-toxic, inexpensive and widely available. Sensible heat storage with water as a storage medium is the most used storage type in combinations with DH systems [13]. TESs can be classified according to several criteria: storage duration (seasonal and short-term TES), storage material (sensible, phase change, thermochemical heat storage material), temperature, position in the heating network (centralized or distributed storage).

3.2 Distributed thermal energy storages

The aim of the internship is to analyze the benefits in using distributed storages in the DHN. In general, thermal energy storages can provide peak shaving and load shifting in DHSs over a time period from one hour to up to a few days, and hence enable a flexible load shape in the system [15]. Specifically, distributed TES are a collection of individual storage units decentralized with respect to the central plant (Figure 5).

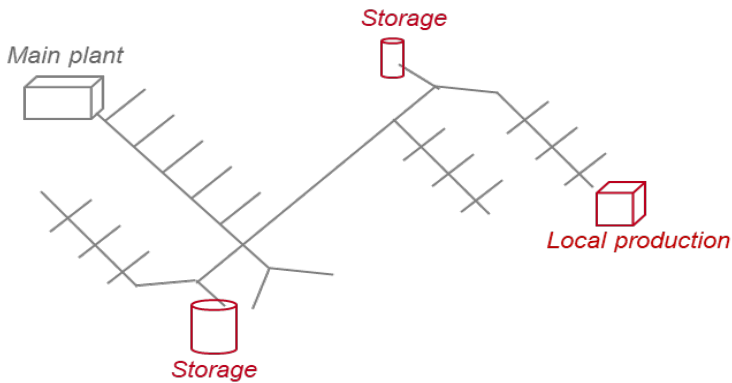


Figure 5. Distributed thermal storages in a DHN.

As the storages are located closer to the substations, the power does not need to be transported from the source to the substation location during the network peak demand. Distributed storages are used to reduce the source power and to reduce the mass flow rate through the bottlenecks in the DHS

during the heat demand peaks. On the other hand, the disadvantage is the fact that distributed storages are more costly for the same total storage size if compared with centralized storage.

3.3 Design parameters and operational principles of a TES

A typical DH storage tank is a steel cylinder that contains water at various temperatures. The structure of a DH tank essentially consists of a series of prefabricated components, assembled on the construction site to form a large cylinder. The two most common materials are steel and pre-stressed concrete. It is also quite common for the main structure to be coated with a layer of stainless steel, generally facing the water. The natural purpose of this layer is preventing the corrosion of the main structure, and, especially in the case of concrete tanks, preventing leakage and vapor transport. When leaks happen, the main effect is the degradation of the insulation layer that can cause a long-term energy loss. The shape of the cylinder is generally advised to be such that the height is larger than its diameter. The values of the aspect ratio (height to diameter) encountered in the literature are typically between 2 and 3.5 [16]. Around the cylinder, a layer of insulating material is wrapped. Common insulants include polyurethane, glass wool, expanded polystyrene, foam glass, and extruded polystyrene.

Sensible TES is a tank in which the water is at different temperatures, typically without mixing completely. This allows the energy content of the storage to change while keeping the amount of water constant. Due to the lower density of the hot water with respect to the colder water, hot water will stay in the upper part of the tank, and the cold one will stay in the bottom. It is important to prevent that the warmer water, that has to be supplied to the customers, will be mixed with the rest of the liquid, which would conserve the amount of energy but destroy exergy and reduce the thermodynamic quality of the heat provided. The concept of separating the two fluids is called stratification; in order to ensure a good stratification a parameter that has to be carefully chosen is the ratio of height to diameter. The design of TES systems essentially aims at averting two main kinds of losses (while minimizing cost): energy losses caused by heat transfer through the external surface, and exergy losses caused by energy transfer inside the tank. It has been observed that in unmixed water tanks it is possible to identify two regions of relatively homogeneous temperature that correspond to the two main temperature levels of the tank content, separated by a region called a thermocline or separation layer or transition zone.

The storage is charged when hot water is supplied from the supply line in the DHN to the top of the tank through a plate diffuser, while the same amount of cold water is drawn simultaneously from the bottom of the tank. Sensible heat storage is characterized by a constant water mass principle, that implies that the temperature of the water changes, depending on the energy content in the tank, but the mass of water remains constant (the amount of hot water that goes into the tank is equal to the amount of cold water flowing out). The efficiency of the stratification depends on the way in which diffusers are designed; during the discharging/charging of the tank, the separation zone moves up or down. The design of the thermal storage requires considerations about operational characteristics, flow, return temperatures and pressure levels of the network in which it has to be integrated. The storage temperature differs from that of the ambient; this leads to have heat losses, so it is important to choose the correct material with adequate mechanical properties and geometry parameters to reduce losses.

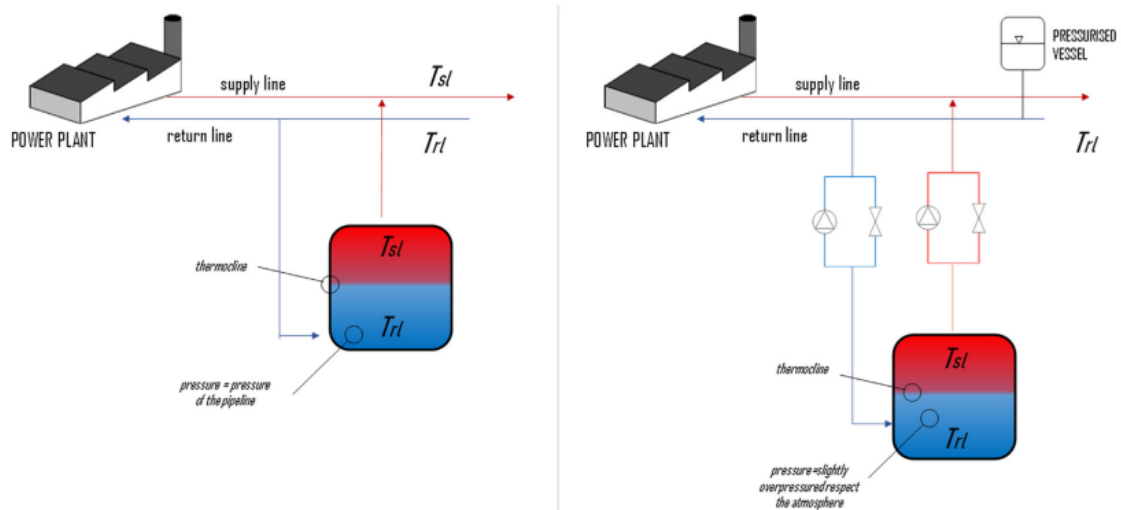


Figure 6. Directly connected storage and pressure-separated storage. [14]

For what concerns the connection with the network, storages can be connected either directly or in a pressure-separated configuration (Figure 6). Storage must be designed as a pressurization vessel when it is connected directly to the network: it will absorb the volumetric variations due to the changing temperatures in the network. Charging and discharging of the storage unit is controlled autonomously depending on the specific differential pressure between supply and return line [12]. If the storage is connected to the network decoupled from the static pressure, a dedicated pressure vessel is as usual required to allow for volumetric expansions/contractions. In this case, the flow in and out of the tank is controlled actively by utilizing a pump and a valve configuration. The water content in the tank is maintained constant controlling either pump in correspondence to the desired heat rate in or out of the storage, while the other pump has a mirror function, where the flow rate is temperature compensated according to the primary pump, thus balancing the amount of water in the storage. Several pressure-separated storage units may be installed in the same network, given that they are decoupled from each other.

The main operational features of TES systems are:

- Energy storage capacity
- Storage time
- Charging and discharging rate

Among these parameters, the energy storage capacity is the most dominant one and it is calculated as follows:

$$Q_{TES} = \rho \cdot c_p \cdot V_{TES} \cdot \Delta T \quad [\text{J}]$$

Equation 2

Where ρ is the density of the fluid inside;

c_p is the specific heat of liquid water;

V_{TES} is the volume of the tank;

ΔT is difference in temperature of the cold and the hot fluid.

Chosen the storage time, i.e. the time in which the storage is fully charged or discharged $t_{ch,disch}$, it is possible to evaluate the mass flow rate needed in order to exchange the desired amount of heat $Q_{ch,disch}$, having assumed a certain temperature difference between the injection and extraction of hot water on one side through the formula:

$$\dot{m} = \frac{Q_{ch,disch}}{c_p \cdot \Delta T \cdot t_{ch,disch}} \quad [\text{kg/s}]$$

Equation 3

3.4 Storage tank model

There are many different types of storage tank models, with different degrees of complexity. To study the dynamics of water injection and extraction, and more generally the functioning of a tank and the details of its hydraulic design, three-dimensional models with CFD software are generally used. However, these models are too complex for studying the use of hot water tanks in the much larger context of a DH network. Often, in large plants, a zero-dimensional model of the individual components and machines is used. In the case of a storage tank, the balance of energy and mass flows exiting and entering the control volume would give as a result, for every instant in time, a single value of the mass and enthalpy contained inside, and of course a single value of temperature, which would be an average for the whole tank. As common as zero-dimensional models are in the analysis of large energy systems, they do not take into account the gradients of properties inside components, which in the case of hot water reservoirs are a fundamental characteristic. An average value of temperature, for example, tells us how much energy is contained inside a volume, but nothing about the thermodynamic quality of the heat that can be extracted or about the mass flow rates needed to exchange a certain heating power. For this reason, one-dimensional models are needed. They study the evolution of parameters along the vertical axis and provide a sufficient level of detail on the water situation. In one-dimensional models, there is no variation of properties in the horizontal plane of the Cartesian representation.

3.4.1 Model in DistrictLab-H

The model of the storage in the simulator DistrictLab-H is a thermo-hydraulic modeling element with walls and it is finite volume discretized. It represents a system composed of a distribution pipe hosting, at its center, one heat storage module. Physical details about the model are listed:

- 1D convection in the fluid;
- Axial conduction in the fluid + mixing term if thermal profile is reversed;
- Wall-fluid thermal exchange;
- Wall: transverse and axial conduction;
- Insulated layer: transverse conduction.

The geometry of the heat storage module is defined relying on the combination of elementary sections (Figure 7). Each section comprises three concentric domains respectively representing the fluid, the wall and an insulation layer. Wall and insulation layer thicknesses can be chosen independently for each section, so continuity is not expected for these variables across the interfaces between two consecutive sections.

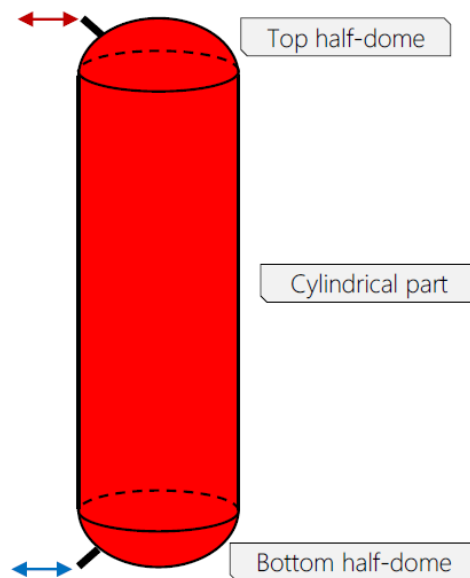


Figure 7. Schematic representation of a heat storage model

The heat storage module is systematically equipped with 20 sensors measuring the fluid temperature at various elevations within the heat storage module. By default, these sensors are equally distributed along the heat storage module, the first (respectively last) element corresponding to the top (respectively bottom) of the heat storage.

3.5 Simulation of TES

As an initial usage example of the model in DistrictLab-H, parameters are set to describe the geometry of the heat storage module:

- Insulation layer thickness
- Wall layer thickness
- Diameter of the tank
- Height of the tank

Other parameters are set to describe the thermal characteristics (thermal conductivity of the insulation layer, thermal inertia, and thermal conductivity of the wall material). The mass flow from the supply line through the tank top is supposed to be exactly the value required to fully charge the storage in ideal conditions. The network, on the other side, always withdraws the same mass flow from the tank bottom layer. The storage volume is 110 m³ and the time to fully charge the storage is equal to the time to fully discharge it (i.e., three hours).

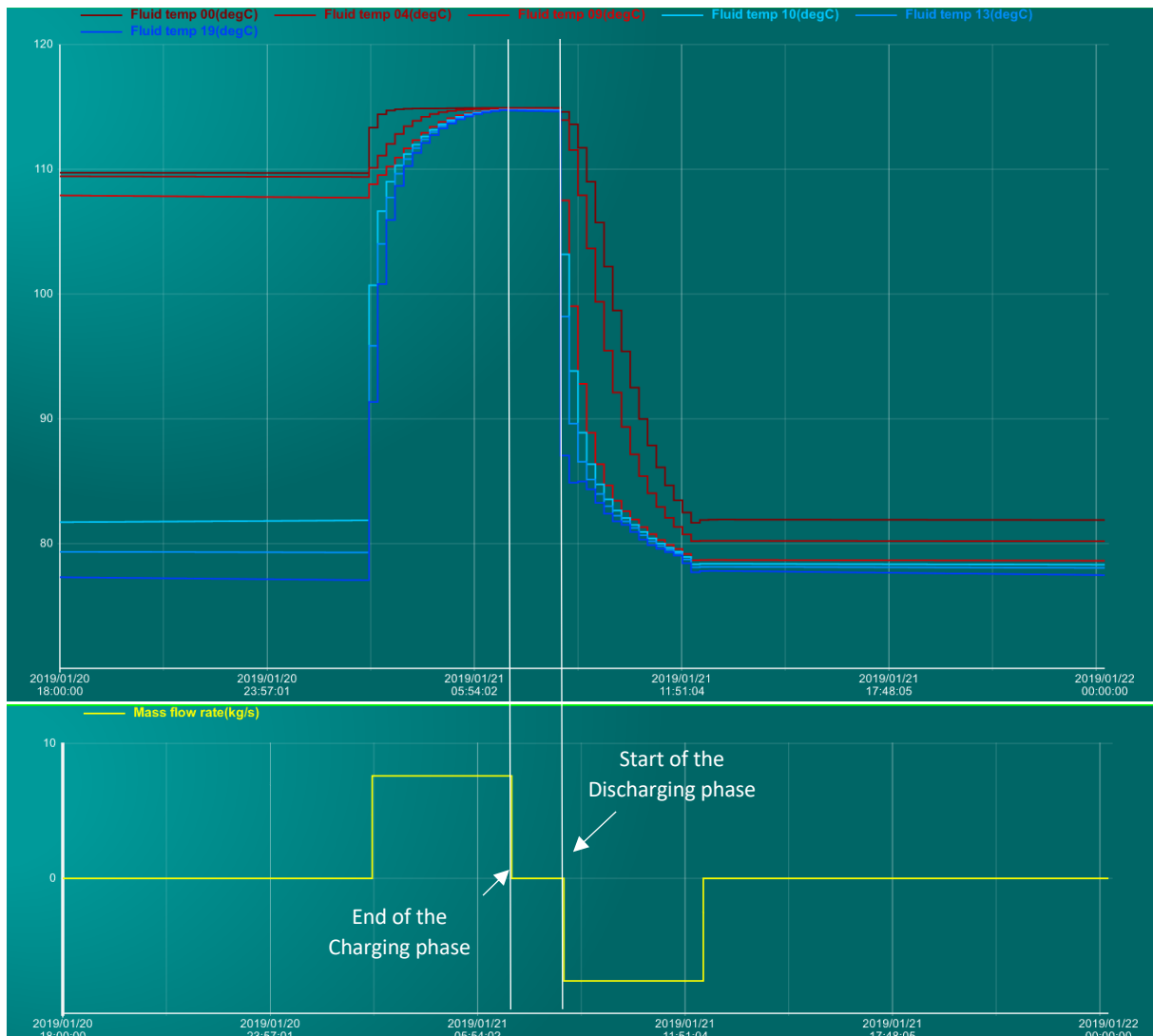


Figure 8. Temperature distribution of six sections of the storage; mass flow rate during charging/discharging phase.

Figure 8 shows the results of the simulation concerning the temperature profile of the storage during charging and discharging phase (highlighted by the bottom part of the graph that shows the profile of the mass flow rate that flows through the tank). Every curve of the top part of the graph corresponds to different horizontal sections of the tank. The mass flow rate introduced in the tank has a temperature of 115°C, after three hours (charging time) all the sections of the storage have the same temperature, independently from the initial conditions (due to the fully charge). During the discharge, the different layers of the storage are cooled down at different rates. As highlighted here, the 1D modeling allows properly catching the thermocline region and highlights the stratification phenomenon.

4. Case study Setup

The aim of the present work is to analyze the behavior of the storage integrated in a DHN and to demonstrate the benefits that a distributed TES can bring to a DHN, in the context of studying retrofitting solutions of existing 2DHN to achieve the goal of lowering the temperature. With the objective of studying the operation of a DH system with and without TES, the present work has been applied to the realistic context of a part of a DH network in the city of Metz (France). More specifically, a set of distributed heat storage has been integrated into a detailed model of the whole system.

4.1 Network description

The Metz DH network is a second-generation DH network that operates at a typical primary temperature level ranging between 100°C and 160°C. The network used in the case study is a simplification of the real one (subnetwork); this subnetwork is connected to the main one through feeder pipe equipped with a pump that is substituted here by a fictitious production site (Figure 9).

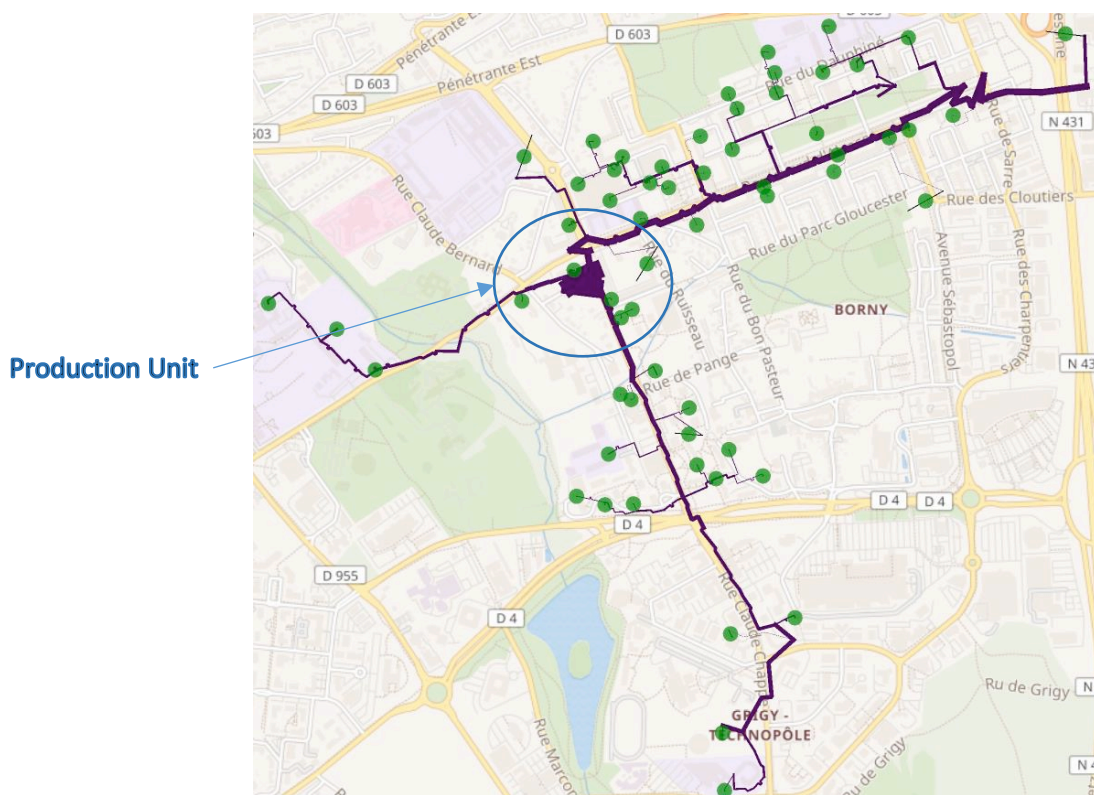


Figure 9. DH subnetwork of the city of Metz

The network is composed of:

- 3 main branches (total length of the network \approx 19.4 km)
- 60 substations (SST)
- 278 piping sections (139 supply, 139 return)
- 279 hydraulic nodes
- 1 thermal and hydraulic production unit

The production unit comprises a heat generator with a considered fixed supply temperature of 157 [°C] [3] (corresponding to the highest value in real operation data from 2021) and a pump, set to maintain a minimal head of 1 [bar] at every substation in the network. The maximum attainable

pressure with the current hydraulic pumps is assumed to be 15 [bar]. The present scenario describes the real network operation during the coldest day in the 2018-2019 heating season: January 21st. The figure below shows the heat demand profile in all the SSTs of the network, that peaks at 46 [MW], and the profile of the external temperature (Figure 10).

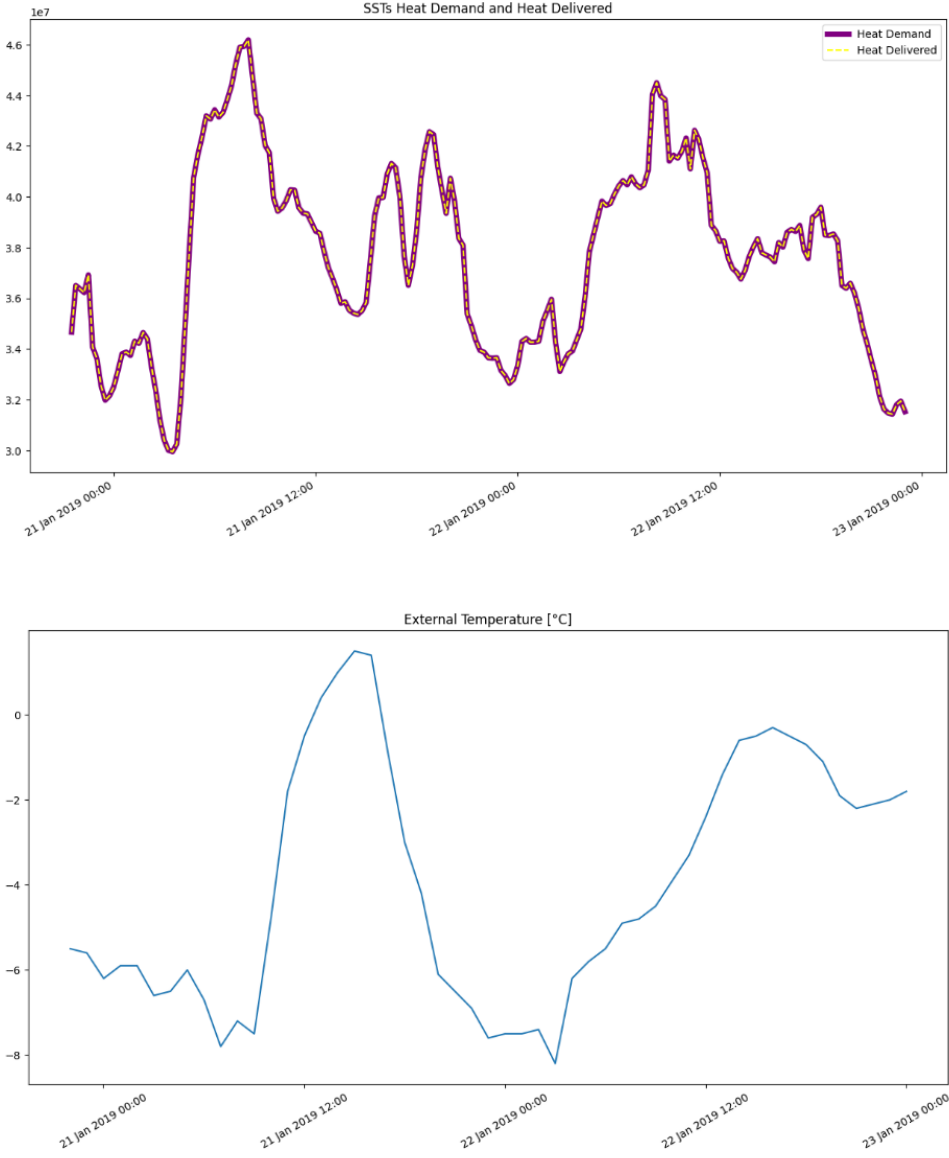


Figure 10. Above: Heat demand profile and the transferred heat. Below: External temperature profile.

4.2 Methodology to identify the bottlenecks

Based on the literature, a methodology to identify the bottlenecks in the studied network has been applied [10]. With respect to other studies [11] that provide a way to address bottlenecks through quantitative criteria, without prioritizing the type of limitation to tackle, here the areas of interest are identified through the following criteria:

- The linear pressure loss in each pipe;
- The water velocity in each pipe;

- The simulated differential pressure at each substation;
- The critical temperature.

For completeness, the critical temperature is the minimum limit for the inlet temperature, under which it is not possible to exchange the required amount of heat, independently from the selected mass flow rate. This parameter is also associated to a given differential pressure at the substation. In the simulated case, the value of the pressure, set by the central pump, is 1 [bar].

The scenario chosen here to simulate the behavior of the network for a lower temperature is based on the assumption of a fixed primary inlet temperature of 115°C. The Figures 11, 12, 13 and 14 show results from the simulator highlighting the behavior of the network according to the chosen criteria at a peak demand: 9 a.m. on the January 21st.

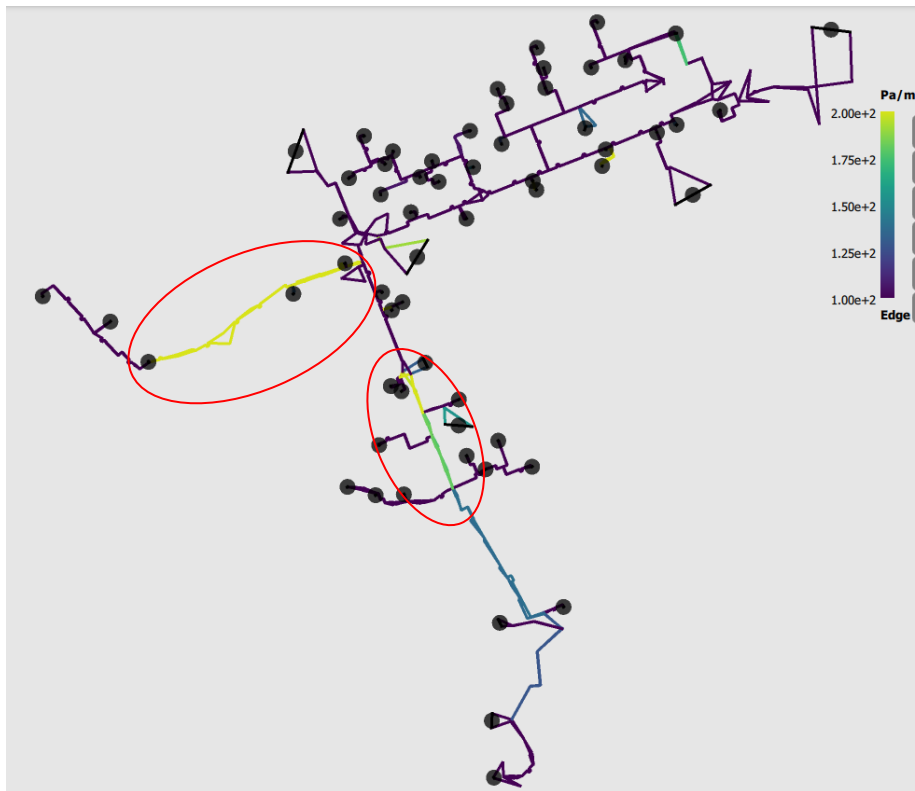


Figure 11. Linear pressure losses

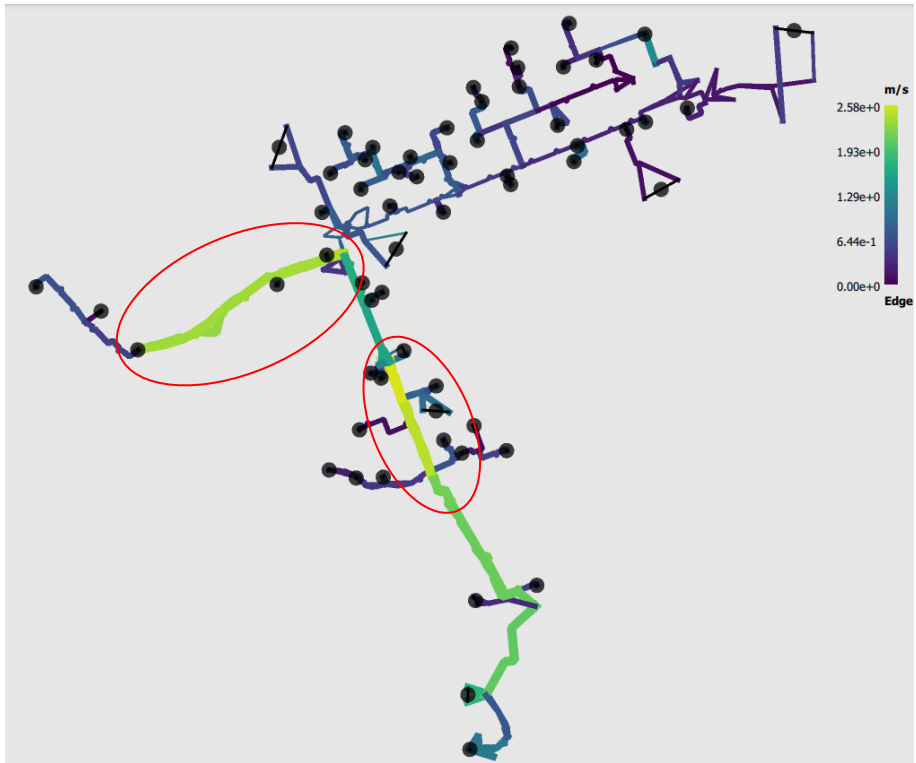


Figure 12. Velocity along the pipes

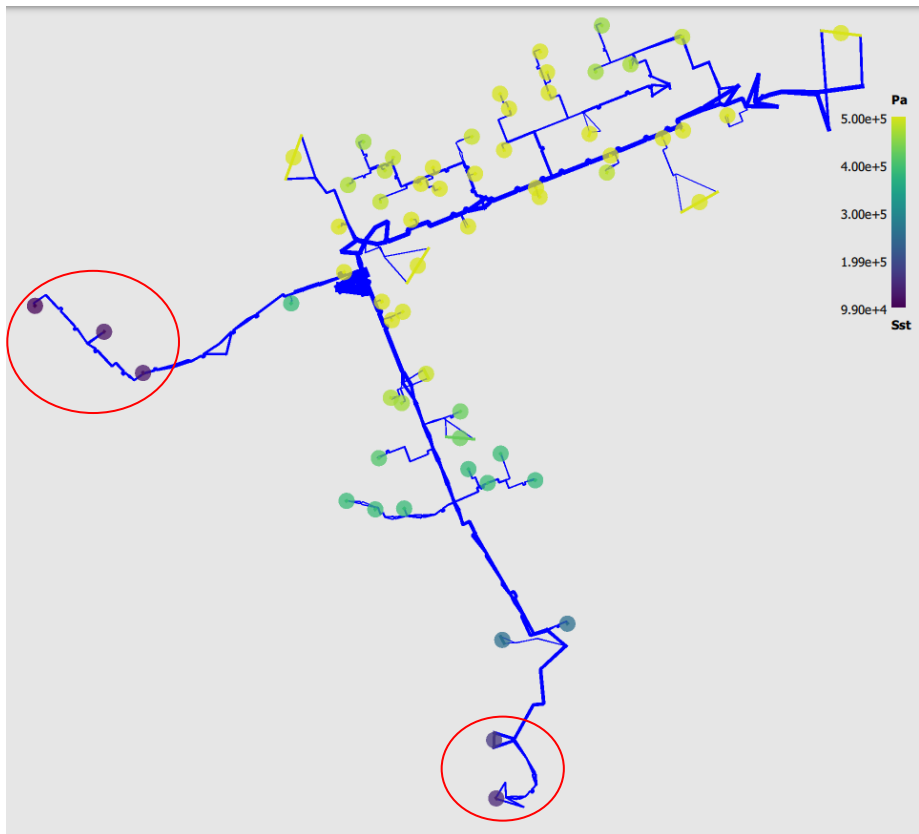


Figure 13. Minimum differential pressure at each substation

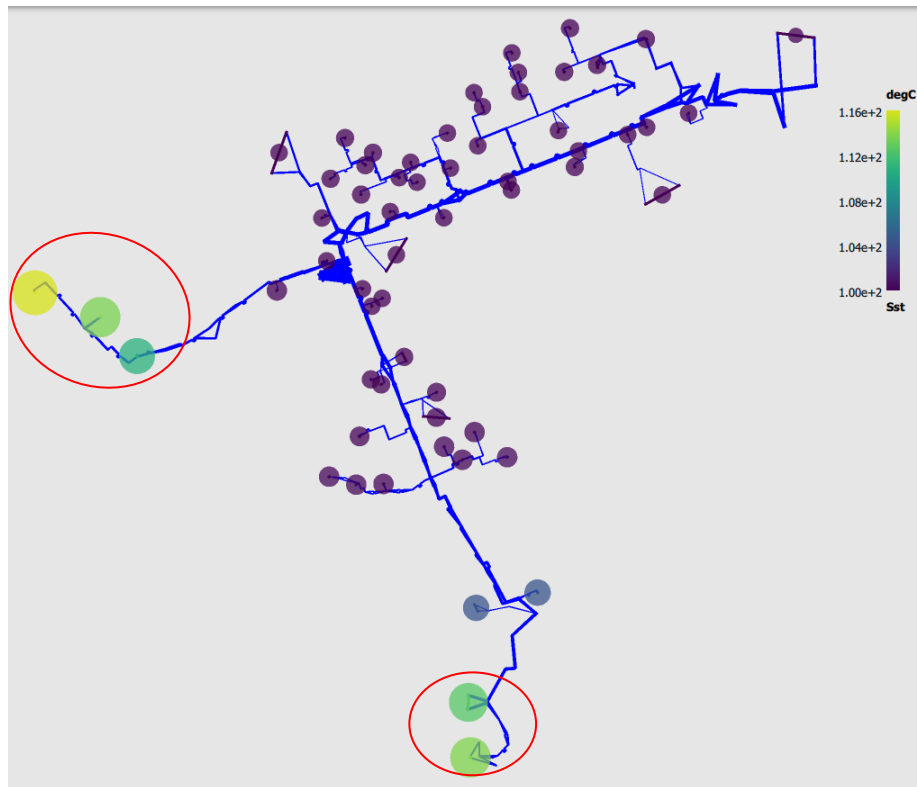


Figure 14. Critical temperature

From the results, it is possible to identify the main sources for the limitation. It is shown that the southern and western branches (highlighted by the red circles) are problematic.

As it is shown in Figure 12, the maximum value of the velocity is reached in the southern branch (maximum velocity is 2,58 [m/s]), this value is critical in terms of pipe fatigue and for the risk of water congestion in pipelines. This area corresponds with the area in which branches have the highest value of pressure losses, in this case the exact value is 200 [Pa/m], as it is clear in Figure 11.

Moreover, at the end of the western and the southern branches, there are five SSTs that show a critical behavior. The difference in pressure in the critical SSTs is very close to the value set by the central pump (Figure 13). In DistricLab-H, substations are of the indirectly connected type with direct control by two-way valves. The controller and the control valve are in charge of regulating the flow in order to satisfy a setpoint for the secondary outlet temperature. The central hydraulic pump controls the deltaP of each SST, keeping its value ≥ 1 [bar]. Figure 13 shows that the critical SSTs require more pumping energy to the central pump to keep the deltaP at the set value. Furthermore, at the peak demand, in the same SSTs, the critical temperature is 116 [°C], this value is higher than the supply temperature (Figure 14).

4.3 TES integrated in the case-study

The identification of the bottlenecks is an important step in order to analyze which are the best retrofitting solutions to unblock the problem of lowering the supply temperature. The results of the simulation in the section 4.2 are used as inputs to identify the two main areas in which the introduction of a thermal energy storage can be an advantage (green areas in Figure 15). Two storages, STORAGE_1 and STORAGE_5, are located, respectively, at the end of the western and southern branch, close to the critical consumers. STORAGE_2 and STORAGE_4 are located downstream the pipes with higher velocity. STORAGE_3 is a centralized storage.

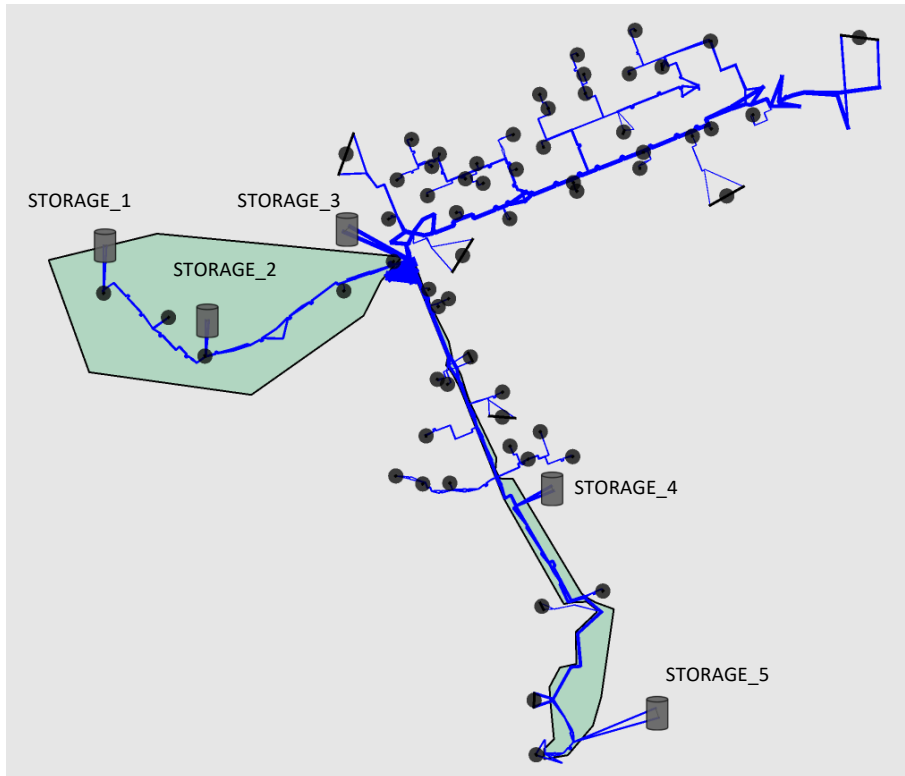


Figure 15. Five TESs integrated in the DHN of Metz

After the choice for the most promising locations of the storage in the network, it is important to consider constraints of the network that have to be met (Table 1) in the design process. Then, preliminary calculations have been done to consistently design the storage.

Table 1. Design Constraints for Storage Location Selection.

CONSTRAINTS

Min differential pressure at each SST	1 [bar]
Min velocity along the pipes	0.02 [m/s]
Max velocity along the pipes	2.5 [m/s]
Max pressure at each node	15 [bar]

Starting from the hypothesis that storages are important when water congestion is a limitation in the context of lowering the temperature of network, the first step of the design process is to consider the velocity target to be reached in each pipe: $vel_{MAX} = 2.5$ [m/s] (Table 1). Having fixed the geometry of the pipes, the velocity is proportional to the mass flow rate (as it is shown in the equation 4), so that the mass flow rate that will flow inside the storage corresponds to the difference in between the mass flow rate of design and the new mass flow rate, proportional to the velocity target.

$$\dot{m} = \rho \cdot \frac{\pi d_{branch}^2}{4} \cdot v_{MAX}$$

Equation 4

Based on the chosen storage discharging time t_{disc} , the desired volume of the storage is calculated as follows:

$$Vol = \frac{\dot{m} \cdot t_{disc}}{\rho}$$

The following section shows the influence of the location and the size of the storage in the context of meeting the constraint of the maximum velocity.

4.3.1 Favorable position and sizing

This case describes the behavior of the network when STORAGE_4 is activated (Figure 16). The operational temperature of this simulation is 115 [°C] and the storage has been assigned a capacity, in terms of [m³] of storable water, that is $Vol = 110$ [m³].

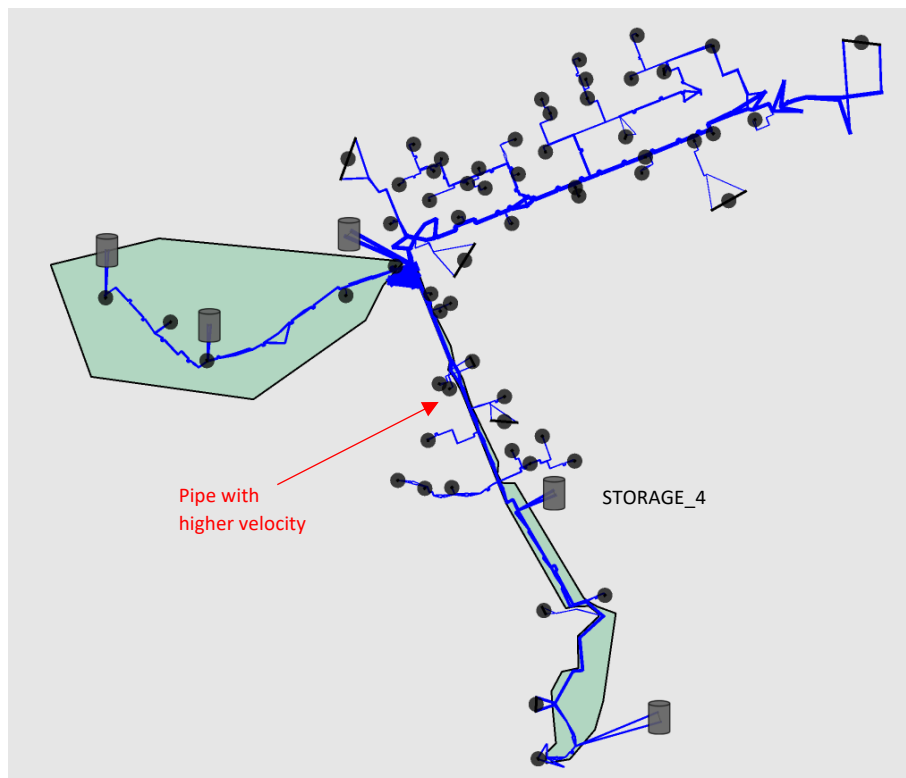


Figure 16. Configuration of the network for the simulation "Favorable position and sizing"

The storage time has been chosen in order to encounter the hypothesis of full charge and full discharge with a fixed agenda as described below:

- Charging time → from 3 to 7 a.m.
- Discharging time → from 8:30 to 12:30 a.m.

The time slot for the discharging phase has been chosen so that the peak demand corresponds with the first hour of discharging, in which the quality of the energy (temperature) transferred by the storage is higher. Figure 17 shows the comparison between the scenario with no storages (purple curve) and the scenario in which the storage is activated (yellow curve). The top part of the graph shows the profile of the velocity of the pipe upstream the activated storage (STORAGE_4) in both scenario; the bottom part displays the mass flow rate inside the storage.

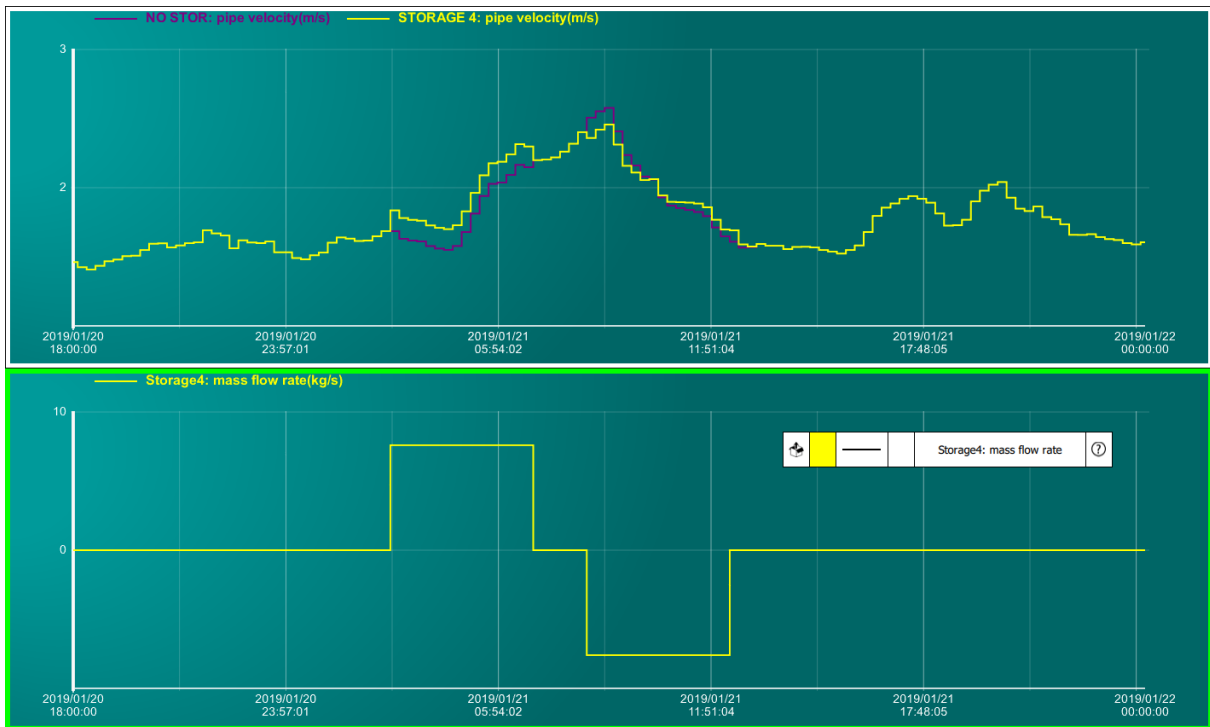


Figure 17. Profile of the velocity [m/s] in the most critical pipe; Mass flow rate [kg/s] inside the storage.

The results show that in the scenario with the storage, the velocity in the critical branch, at the peak demand, is lowered from $v_{\max_{NO_STOR}} = 2,58$ [m/s] to $v_{\max_{STOR}} = 2,45$ [m/s].

4.3.2 Not Favorable position and sizing

Another simulation, here, has been performed. It describes the behavior of the network when STORAGE_5 is activated (Figure 18).

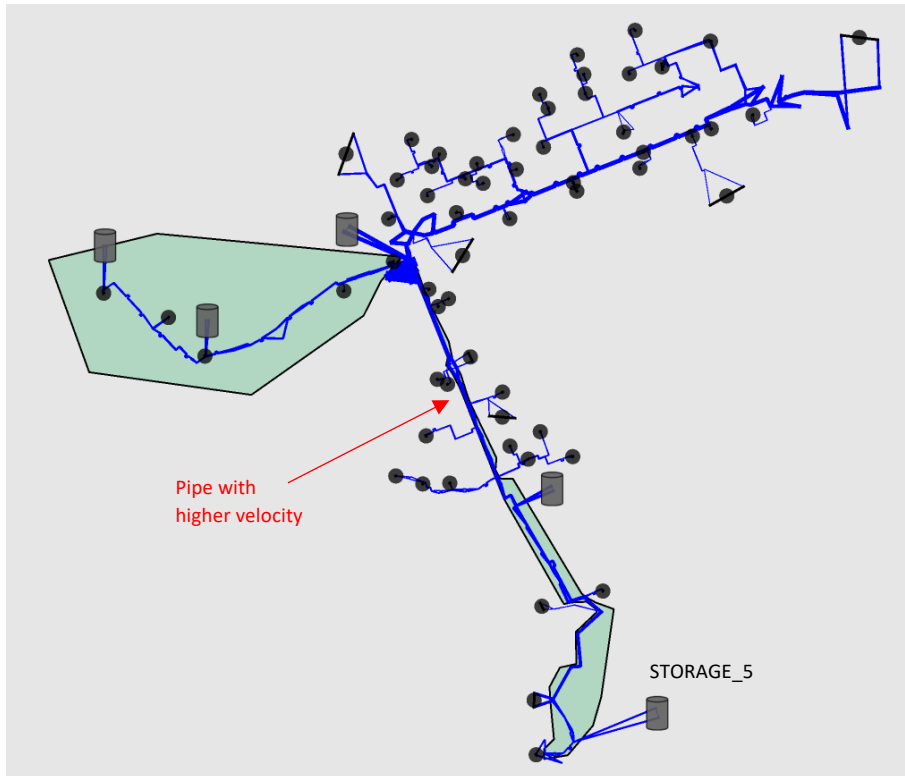


Figure 18. Configuration of the network for the simulation "Not Favorable position and sizing".

For the sake of clarity, we will refer to the simulation as "Simulation A", where STORAGE_5 has a volume of $Vol = 110 \text{ [m}^3\text{]}$; while "Simulation B" is referred to the STORAGE_5 with a volume that is twice bigger than the previous one. In both simulations, the duration for both charging and discharging is fixed at four hours each. Additionally, specific time slots for charging (3:00 A.M. to 7:00 A.M.) and discharging (8:30 A.M. to 12:30 P.M.) are predetermined. The hypothesis of the simulation A is the storage is fully charged and fully discharged during the operating time. The aim is to evaluate the influence of the position of the storage. The results of this simulation are shown in Figure 20. The activation of the STORAGE_5 allows to reach the same target of velocity, but the heat demand constraint is not being adequately addressed.

The bottom graph of the Figure 19 displays the heat demand (purple curve) of the substation downstream the storage and the heat transferred (yellow curve) to the same SST. It is interesting to notice that during the last part of the discharging phase, the heat transferred to the SST is not enough to meet the demand. This gap is due to the fact that the temperature of the fluid flowing out from the storage (purple curve in Figure 20), mixed with the fluid coming from upstream branch, is lower than the critical temperature (yellow curve).

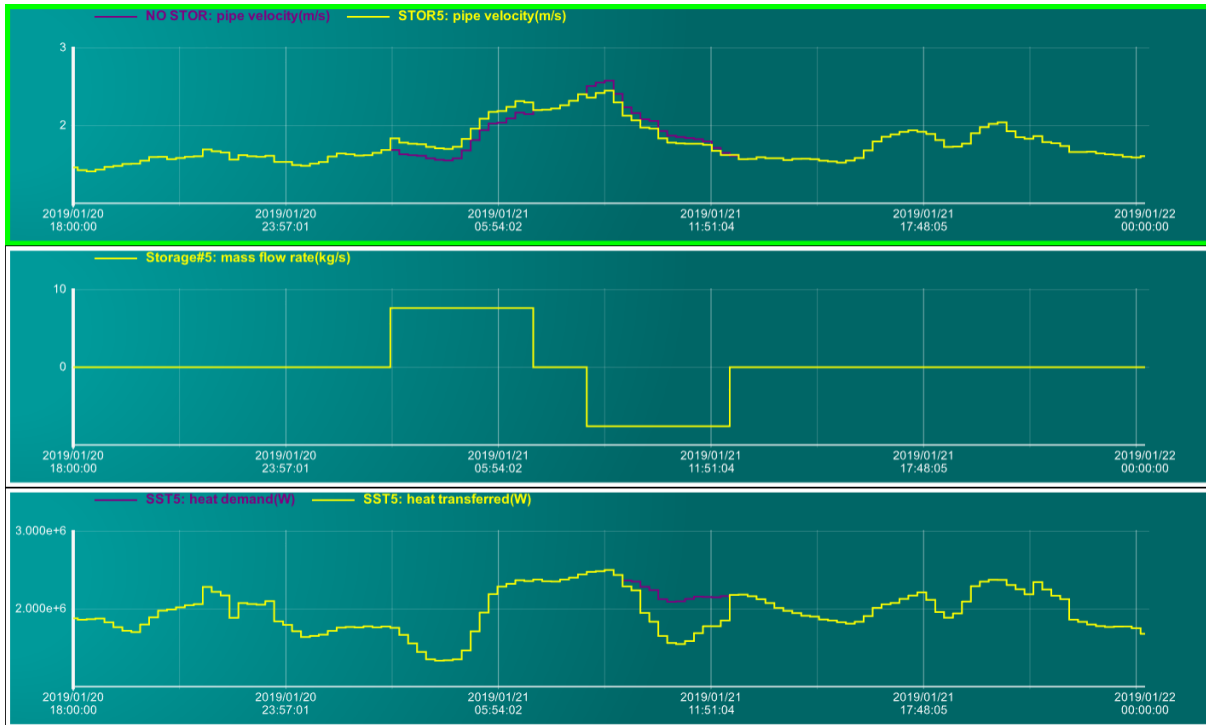


Figure 19. Profile of the velocity [m/s] in the most critical pipe; Mass flow rate [kg/s] inside the storage; SST 5 Heat Demand-Heat Transferred [W].

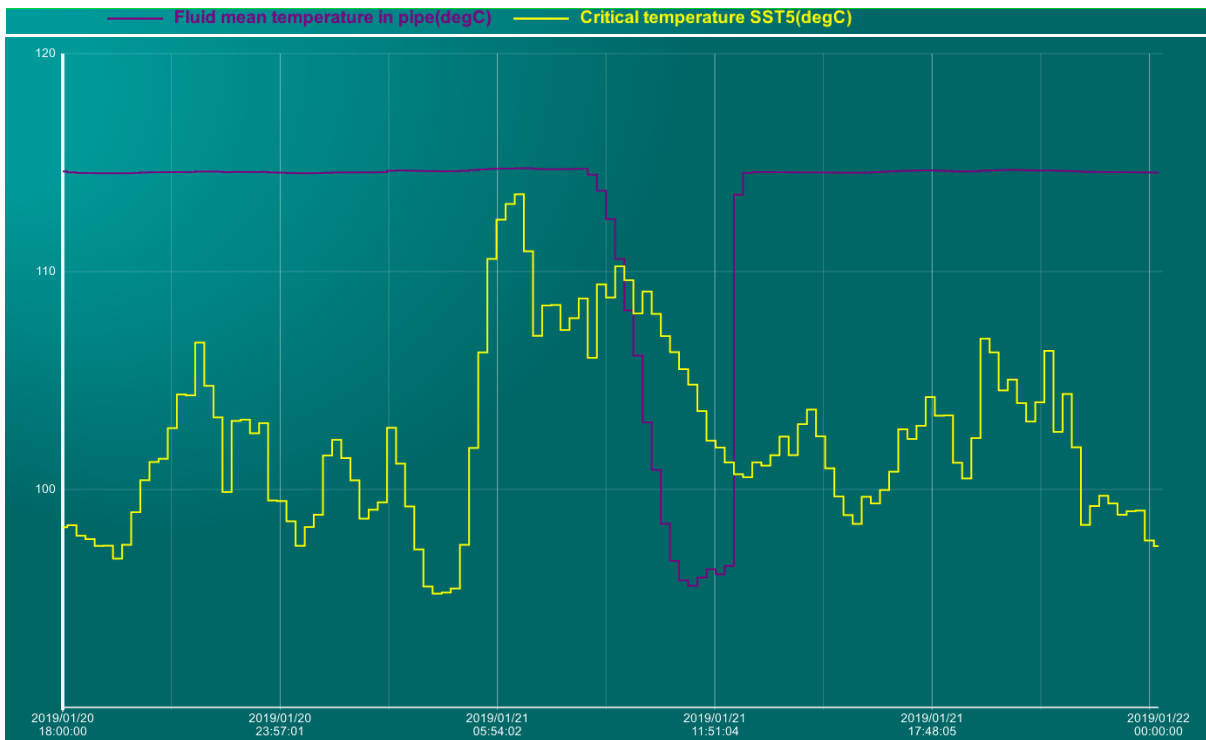


Figure 20. Comparison between critical temperature [°C] of a SST and fluid mean temperature [°C] of the pipe upstream the SST.

As a result, the design of the STORAGE_5 operated as explained beforehand is not optimal. Consequently, new settings on the piloting and the sizing of the storage could be evaluated. In order to overcome the limit of the heat demand satisfaction, the fluid into the SST has to carry more energy

with respect to the previous case. To do so, the new simulation, referred as simulation B, is characterized by a setting of a half charge and a half discharge of a bigger storage, so that the same target of velocity could be reached, keeping constant the mass flow rate flowing into the storage, and only the part of the storage with higher quality of energy is discharged (fluid at higher T).



Figure 21. New simulation: Profile of the velocity [m/s] in the most critical pipe; Mass flow rate [kg/s] inside the storage; Heat Demand-Heat Transferred [W].

In the Figure 21, the green curve represents the behavior of the storage in the simulation B. As it is shown by the upper graph, the velocity profile of the pipe upstream the storage at the peak demand is reduced; it is lower than 2.5 [m/s]. In the bottom graph, the heat transferred by the storage in the simulation B is overlapped on the purple curve (heat demand), so that also the target of the heat demand is met. Indeed, as it is shown by the Figure 22, the profile of the temperature downstream the storage (i.e., the temperature of the fluid directly supplied to the substation), that is represented by the purple curve, is higher than the critical temperature of the substation at the end of the branch (yellow curve), allowing to have met the heat demand.

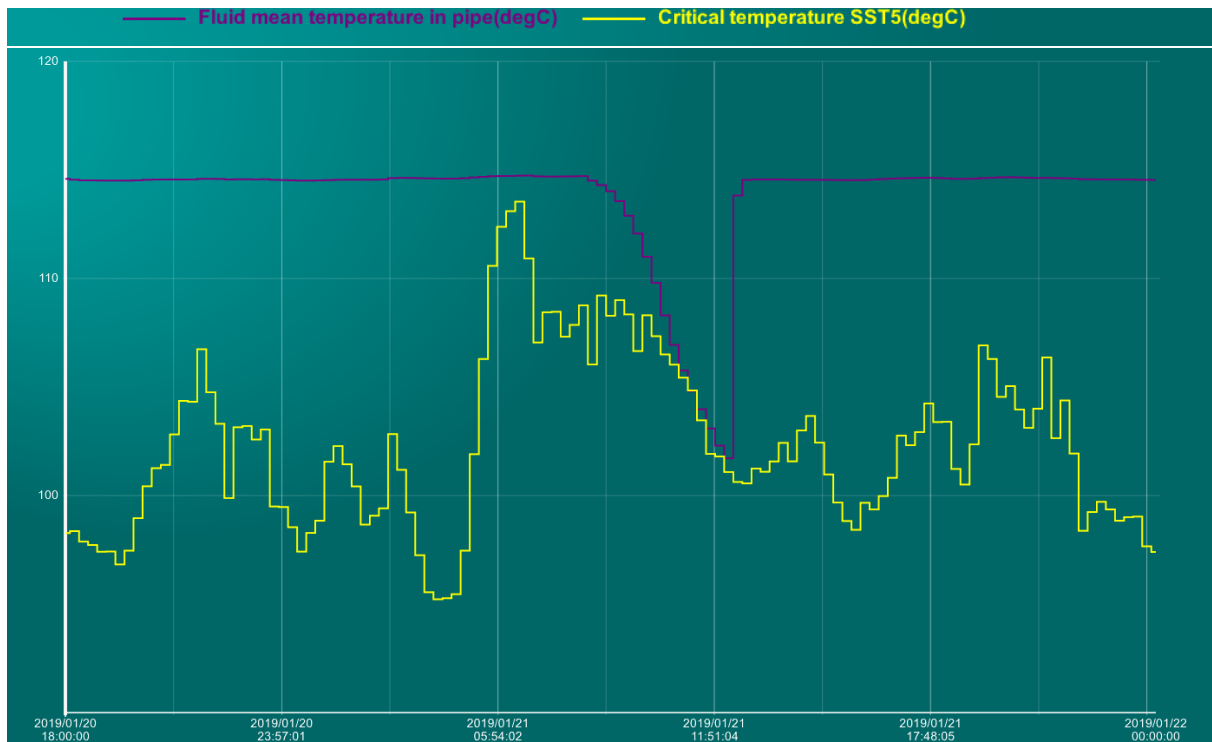


Figure 22. Comparison between critical temperature [°C] of a SST and fluid mean temperature [°C] of the pipe upstream the SST.

4.3.3 Impact of the piloting of the charging phase on the discharging phase

The impact of piloting the charging phase on the discharging phase is a critical consideration in the design and operation of energy storage systems. This dynamic relationship between the two phases plays a significant role in the overall performance and efficiency of such systems. In this section, two distinct scenarios are presented to examine the potential outcomes and implications of different approaches or conditions:

- Scenario 1: during the charging phase the whole volume is charged (fully charged), during the discharging phase only the 50% of the volume is discharged (half-discharged);
- Scenario 2: during the charging phase 50% of the volume is charged (half-charged) and also during the discharging phase only the 50% of the volume is discharged (half-discharged).

It's important to note that only STORAGE_5 is in operation during these scenarios. The storage time is fixed: four hours for charging and discharging, also the time slots for charging (3:00 A.M. to 7:00 A.M.) and discharging (8:30 A.M. to 12:30 P.M.) are fixed. Analyzing the results from the simulation, in the scenario 2 the SST downstream the storage is fully satisfied (i.e., the heat transferred corresponds to the heat demand), in the scenario 1 this does not happen. The reason is related to the temperature of fluid that comes out from the storage.

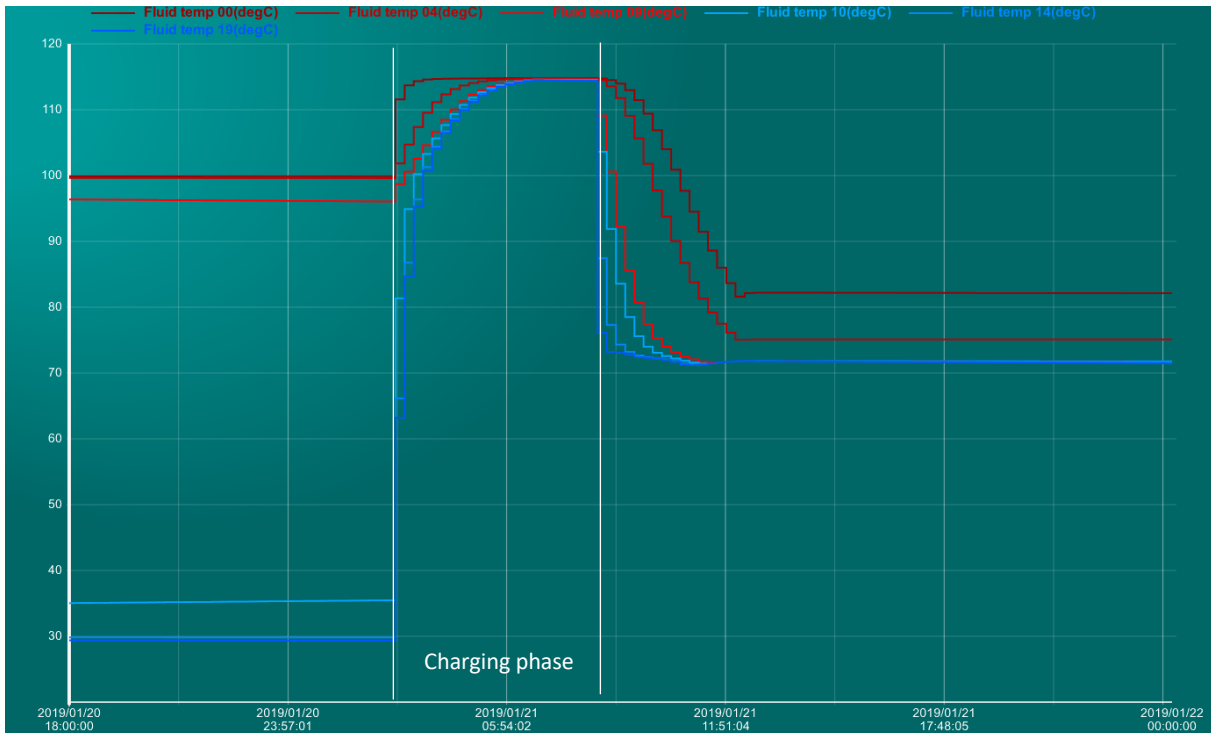


Figure 23. Temperature [°C] profile of six layers of STORAGE_5 in the scenario 1.

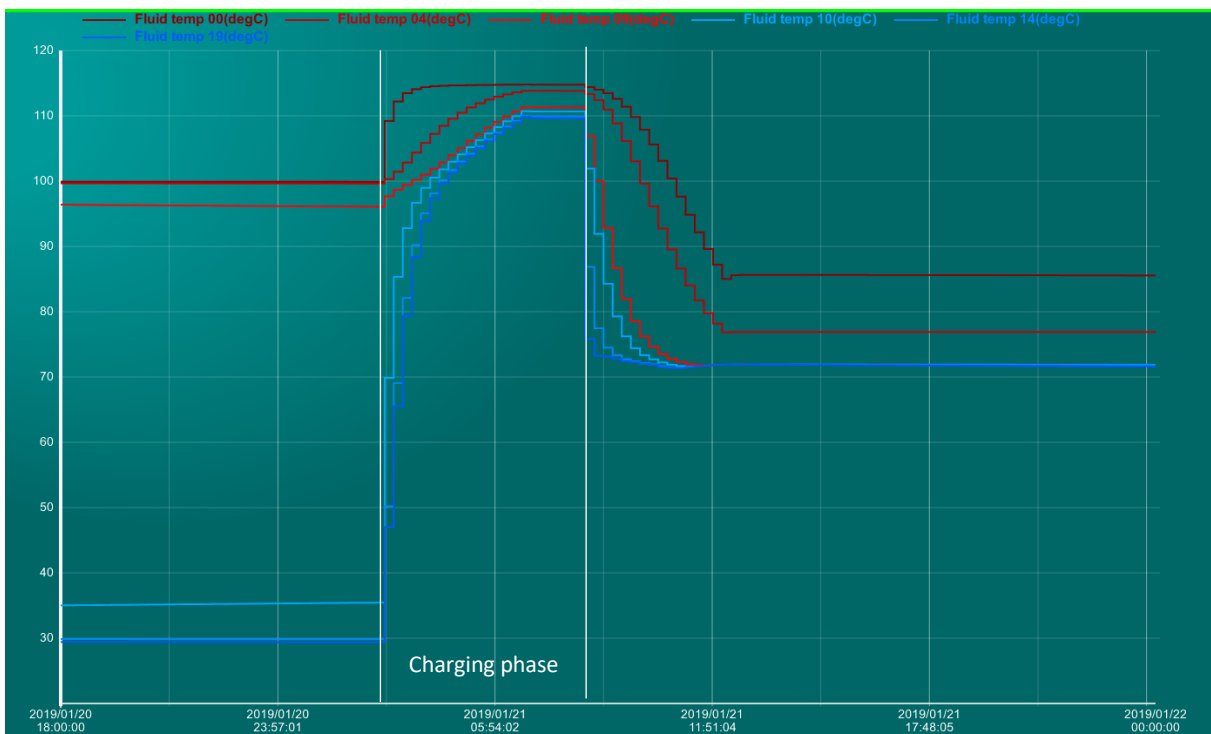


Figure 24. Temperature [°C] profile of six layers of STORAGE_5 in the scenario 2.

As it is noticeable from Figure 23 and Figure 24, the temperature distribution inside the storage is not the same in both scenarios. In the scenario 1, all the layers of the storage reach the temperature of the supply line (fully charged) at the end of the charging phase; on the contrary, at the end of the charging phase, in the scenario 2, the top layer has a temperature of 114,8 [°C] and the bottom layer is at 109,6 [°C]. Analyzing the average of the 10 top layers of the storage at the end of the charging

phase (Figure 25), the average temperature in the scenario 1 is higher with respect to the one in scenario 2. During the discharging phase, this behavior is inverted and this is the reason why the storage in the scenario 2 can satisfy the heat demand of the SST that is downstream.

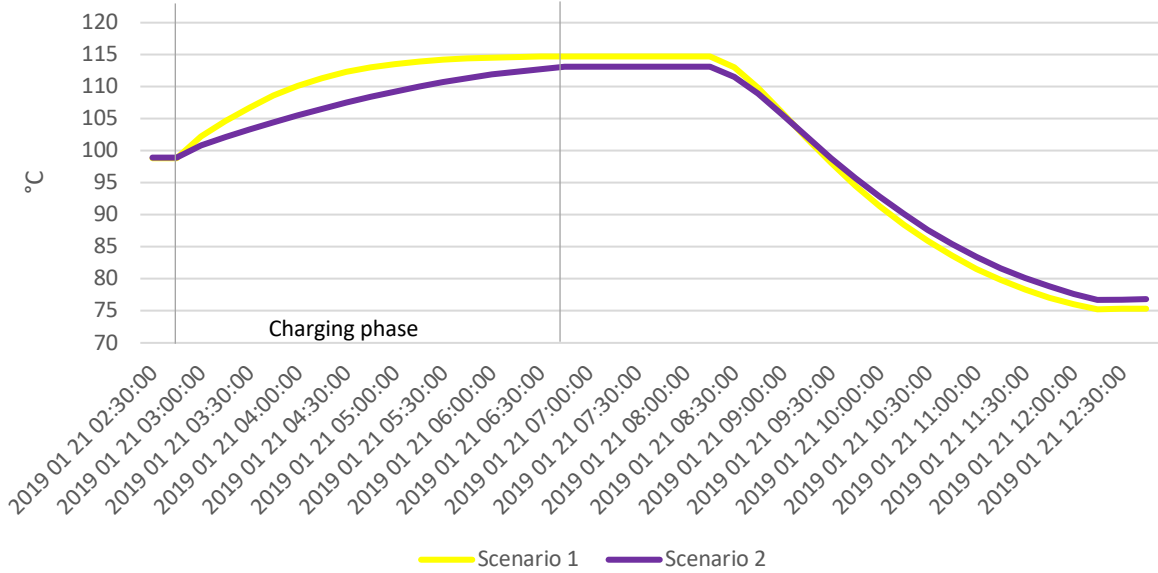


Figure 25. Average temperature of the first 10 top layers of the storage during the discharging time.

This inverted behavior is due to the convection in between the fluid coming from the return line, that has the same value in both cases, and the fluid inside the storage. In the scenario 1, the fluid from the return line exchanges heat with the entire volume, that is at uniform temperature. Here, there is a global and efficient convection in the fully charge storage that leads to circulation of fluid in the whole volume. In the scenario 2, the fluid from the return line will be mixed with the bottom layers that are at a lower temperature, while the top layers will be discharged in the supply line, releasing a greater amount of energy. Here, natural convection is less efficient, it is prevented by the stratification. This behavior has to be taken into account during the process of parametrization of the storage in an optimization problem.

5. The Optimization Process

Energy consumption reduction in buildings features various efficiency measures in heating systems and in DHN. As DHNs evolve towards lower temperatures, the design of such systems is more complex and it is crucial to maintain a high thermal and economic performance.

5.1 Characteristics of the Optimization

Optimization is a mathematical and computational process used to find the best possible solution or outcome from a set of possible choices or alternatives. It is a fundamental concept in various fields, including mathematics, engineering, economics, computer science, and many others. The goal of optimization is to maximize or minimize a specific objective or criterion, subject to a set of constraints. Optimization typically involves defining an objective function or a cost function that quantifies the performance or quality of a solution. The goal is to either maximize or minimize this function, depending on the problem. In the multi-objective optimization (MOO), there are two or more objectives that you want to optimize. These objectives can be related to different aspects of a problem, and they may have different units of measurement or scales. MOO addresses this complexity by attempting to find a set of solutions that represent a trade-off among these conflicting objectives (Section 5.1.1). The optimization problems involve decision variables, which are the variables that can be adjusted or controlled to influence the objective function. The feasible solution space often is limited by constraints, that can be equations or inequalities that restrict the values the decision variables can take. These constraints reflect real-world limitations and practical considerations. In some cases, optimization aims to find the best solution within a specific region of the solution space (local optimization). In other cases, the goal is to find the absolute best solution across the entire solution space (global optimization). Solving optimization problems often involves iterative methods. Various algorithms, such as gradient descent, genetic algorithms (Section 5.1.2), and linear programming, can be used to search for optimal solutions by iteratively adjusting the decision variables. To tackle this complex optimization problem, metaheuristics is used. Metaheuristics are optimization techniques that don't rely on explicit mathematical formulations of the problem. Instead, they explore the solution space in a heuristic manner, making educated guesses and refining solutions iteratively. Popular metaheuristics include genetic algorithms, simulated annealing, particle swarm optimization, and others. Metaheuristics iteratively search for solutions by evaluating the performance of various candidate solutions generated through a combination of exploration and exploitation strategies. These methods are particularly useful when dealing with complex and non-linear problems, where analytical optimization is challenging.

In summary, an optimization problem is characterized by the types of variables, the linearity or not of the equations (objective function and constraints), the number of objective function and the consideration of the time (time-related factors, such as dynamic behavior, temporal constraints, or time-dependent objectives).

5.1.1 Multi-objective optimization

Consider a decision-maker faced with a complex optimization problem involving multiple objectives, each of which needs to be minimized. These objectives are often non-commensurable, meaning there is no clear preference for one objective over another. In real-life scenarios, these objectives often conflict with each other, and optimizing for one may lead to undesirable outcomes for the others. Therefore, finding a single solution that optimizes all objectives simultaneously is often impractical. Instead, a reasonable approach is to seek a set of solutions, each of which meets the objectives to an acceptable degree without being dominated by any other solution. In this context, if all objectives are

for minimization, a feasible solution "x" is said to dominate another feasible solution "y" if it performs better in at least one objective without being worse in any other objective. A solution is considered *Pareto optimal* if it is not dominated by any other solution in the solution space. A *Pareto optimal* solution cannot be improved in any objective without worsening at least one other objective. The collection of all non-dominated feasible solutions is called the *Pareto optimal set*, and the corresponding objective values form the Pareto front. However, identifying the entire *Pareto optimal* set is often impractical due to its potentially enormous size, and for some problems, it is computationally infeasible to prove solution optimality. Therefore, a practical multi-objective optimization approach aims to identify a set of solutions that approximates the *Pareto optimal set* effectively. In achieving this goal, a successful multi-objective optimization algorithm should strive for three conflicting objectives:

- The best-known Pareto front should closely approximate the true Pareto front, ideally being a subset of it.
- The solutions in the best-known Pareto set should be diverse and evenly distributed across the Pareto front to provide a comprehensive understanding of trade-offs.
- The best-known Pareto front should capture the entire range of possibilities within the Pareto front, including solutions at the extremes of the objective function space [19].

Overall, multi-objective optimization seeks to strike a balance between these objectives to help decision-makers navigate complex problems with multiple conflicting objectives.

5.1.2 Genetic algorithm

The concept of Genetic Algorithms (GAs) was developed in the 1960s and 1970s by Holland et al. [17]. GAs draw inspiration from the theory of evolution, which explains the origin of species in nature. In the natural world, weaker and less fit species often face extinction due to natural selection, while stronger ones have a better chance of passing on their genes to the next generation through reproduction. Over time, species carrying advantageous gene combinations become dominant, and occasionally, random genetic changes may lead to the emergence of new species with additional advantages. In the context of GAs, a solution vector, denoted as " x_i " is referred to as an individual or chromosome. Chromosomes are composed of discrete units called genes, where each gene controls one or more features of the chromosome. Initially, in the original implementation of GAs by Holland, genes were assumed to be binary digits (0 or 1). However, more diverse gene types have been introduced in later implementations. Typically, a chromosome corresponds to a unique solution in the solution space, and there exists a mapping mechanism, known as encoding, between the solution space and the chromosomes. GAs operate using a collection of chromosomes, referred to as a population, which is usually initialized randomly. As the optimization process unfolds, the population includes increasingly fit solutions, and eventually, it converges, meaning that it is dominated by a single solution. GAs employ two key operators to generate new solutions from existing ones: crossover and mutation. *Crossover* is a fundamental operator in GAs, where two chromosomes (parents) are combined to produce new chromosomes (offspring). Parents are typically selected from the population with a preference for their fitness, aiming to pass on favorable genes to the offspring. By iteratively applying the crossover operator, the genetic makeup of good chromosomes becomes more prevalent in the population, leading to convergence towards a globally good solution. The *mutation* operator introduces random changes into the characteristics of chromosomes, typically at the gene level. The mutation rate (the probability of altering a gene's properties) is usually very small and dependent on the chromosome's length. Therefore, mutations result in minor changes from the

original chromosome. Mutation plays a crucial role in GAs by reintroducing genetic diversity into the population and aiding the search in escaping local optima.

5.2 Optimization method for Storage Location and Size Selection

In order to solve the optimization problem, an optimization framework is used. The methodology features an optimization method combined with a nonlinear evaluation function, using the DHN simulation engine described in section 1.3. The choice of the optimization method has been made considering the main characteristics of the problem, which are the discrete nature of the decisions parameters, the possible amount of decision parameters that can be greater than one hundred, and the non-linear nature of the evaluation function. In multi-objectives optimization (MOO) methods, genetic algorithms (GA) are widely used to solve similar problems. Among GA, many papers show the robustness and the great performance of the specific NSGA-II algorithm in the field of energy engineering [10]. Within multiple implementations, the implementation of the Python library DEAP [18] is used, which features an improvement on the crowding distance calculation, increasing the performance of the algorithm. The optimization process provides an ensemble of individuals, each describing a set of modifications to be performed on the DH network. The evaluation function implements a DHN model including those modifications and to be used with the simulator DistrictLab-H for the evaluation of the performance. The proposed methodology has been presented in previous publications ([19] and [10]). For the former, the only decision variables were the pipe diameters, while for the latter, the possible assets to modify were the pipes diameter, the substations size and booster pumps location and differential pressure.

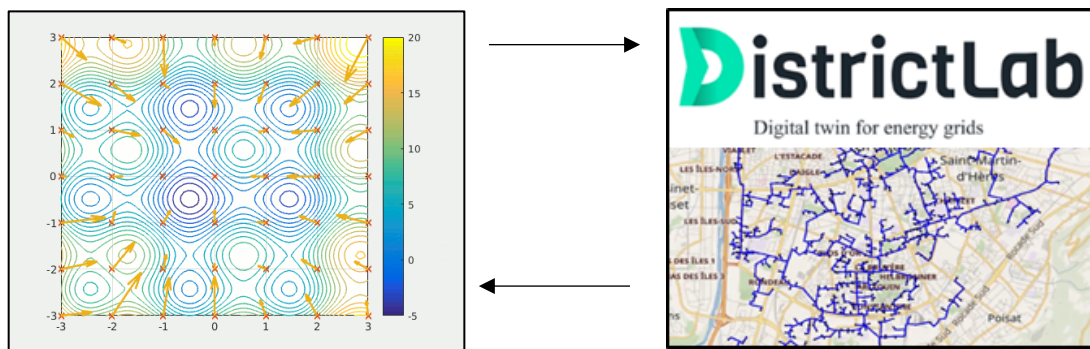


Figure 26. Combination of optimization algorithm (on the left) and dynamic simulator (on the right).

The method is based on the combination of the algorithm for the optimization and the dynamic simulation to evaluate the results (Figure 26). It consists in the initialization of the optimization process, through the GA that create a random population composed by a set of individuals. This is the input of the dynamic simulator, which evaluates the proposed performance of the configuration of the DH network. The outputs of the simulation are new inputs for the GA that create a Pareto curve where, the objective is to minimize the two objective functions, OPEX and CAPEX. In the optimization section, the goal is to present a diverse array of solutions tailored to meet the unique constraints and preferences of the operator. The aim is to empower the operator with the flexibility to select the most suitable solution based on their specific needs, which may include considerations such as construction work limitations, available CAPEX (Capital Expenditure) resources, and other relevant factors. By offering a broad spectrum of solutions, it is intended to provide the operator with the tools necessary to make well-informed decisions that align with their project objectives and constraints.

Any solution to the optimization problem has to verify constraints regarding the satisfaction of the consumers' heat demand, fluid velocity and absolute pressure in the DH network, as shown in Table 2.

Table 2. Constraints for Optimization Problem in District Heating Network Design.

CONSTRAINTS	
Min velocity along the pipes	0.02 [m/s]
Max velocity along the pipes	2.5 [m/s]
Max stagnation pressure at each node	15 [bar]
Heat delivered/Heat demand ratio	> 0.99

The maximum velocity criterion is selected in order to avoid the risk of premature deterioration of the pipes, instead, the minimum velocity is chosen in order to avoid long residence time of the water in the piping system. Maximum stagnation pressure is selected according to technical specifications of pipe manufacturer and the minimum satisfaction rate is selected high but not at 100% to increase the diversity of the proposed solutions (Table 2). When using genetic algorithm, and specifically NSGA2, some hyper parameters describing the population size and mutation rate have to be set. These hyper parameters are listed in the Table 3:

Table 3. Selected parameters for NSGA2 algorithm for the tested cases.

PARAMETERS SELECTED FOR NSGA2 ALGORITHM	
Mutation probability	0.02
Crossover probability	0.8
Population size *	24/80/400
Number of generations *	12/80/200

* the three different values correspond to three different decision spaces

5.3 Integration of storages in the optimization process

The identification of the bottlenecks, described in the section 4.2, is an important step in order to analyze which are the best retrofitting solutions to unblock the problem of lowering the supply temperature. In the existing study [10], the solutions that have been considered are:

- Modifications of piping sections;
- Thermal/Hydraulic re-sizing of the substations located at the end of the critical branches;
- Possible addition of a booster pump.

The added value of this study is to consider another possible solution: the addition of centralized or distributed storages. Distributed TES, more specifically - as described in chapter 3 - can help to solve the problem of the water congestion and to relax the central production unit during the peak time (when the demand is higher).

5.3.1 Decision space

The decision space for this optimization includes four kinds of possible modifications, corresponding to each type of decision variables that are the pipe choices, the substation resizing, the booster pumps position and size and thermal energy storages location and size (Figure 27). Each decision variable corresponds to a discretized set of possible values:

- The discrete decision variables for pipes correspond to a range of standard diameters of the pipes from the DN20 to DN500. The number of pipes that are included in the decision space are 21 and are located in the critical branches (red line in Figure 27).
- The discrete decision variables for substations correspond to an upgrade on the thermal sizing power. This is allowed through a multiplicative factor which ranges from 1.2 to 2 with a 0.2 step. Associated retrofit of the hydraulic elements is performed accordingly using the nominal operating point of the substation as reference. The concerned substations are highlighted with grey big circle on Figure 27.
- The discrete decision variables for the booster pumps correspond to the option of installing a pump with a fixed head gain ranging from 0.5 bar to 3 bar with a 0.5 bar step, for each of the four available locations ('P' tagged circle on Figure 26).
- The discrete decision variables for the TESs correspond to the option of installing a storage with a volume that can varies between the values: 70 [m³], 125 [m³], 196 [m³]. The storages can be installed in five available locations, as shown in Figure 27. The charging/discharging time, the storage time and the percentage of volume charged/discharged are fixed and they are shown in Table 4.

Table 4. Fixed Thermal Energy Storage (TES) Parameters.

Charging time	From 3:00 A.M. to 6:00 A.M.
Discharging time	From 8:30 A.M. to 11:30 A.M.
Storage time	3 hours
Percentage of volume charged/discharged	100 %

The number of possible solutions that characterizes the problem is $5 \cdot 10^{35}$.

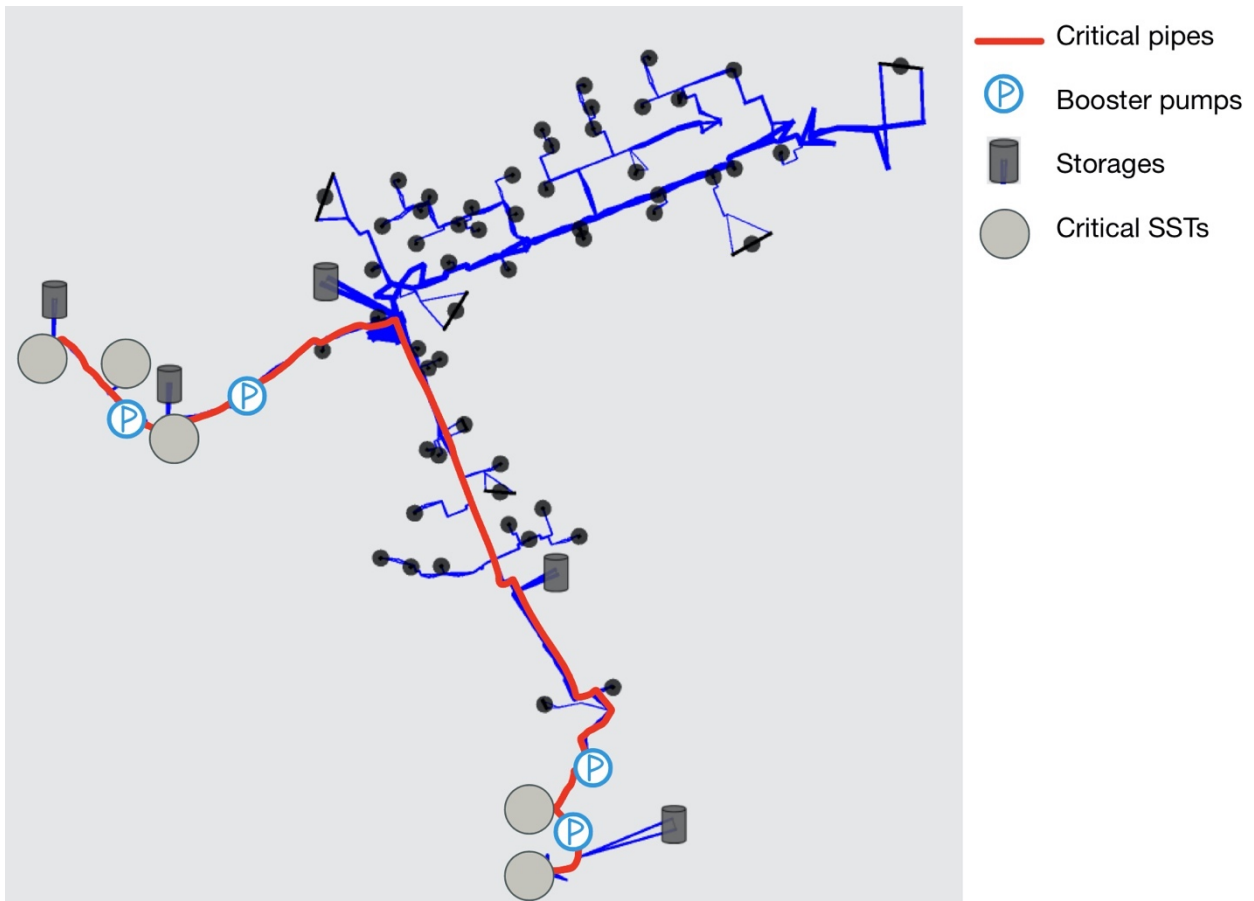


Figure 27. Network with the highlighted elements populating the decision space of the optimization framework.

5.3.2 Objective functions

Each individual design is evaluated with respect to two objective functions: investment costs (CAPEX) and operational costs (OPEX). The CAPEX part corresponds to the sum of the costs for each of the proposed modifications on the network. The corresponding cost structure features a fixed price for each modification and a variable price, depending on the selected decision parameter value. For each modified pipe section, a fixed price of 10 [€/m], in addition to a variable price depending on the selected diameter, is used. For each modified SST, a fixed price, considering the costs related to the power capacity adjustment, and the variable price of 11 [€/kWh] are considered; for each added booster pump, a fixed price is used to account for the installation and the variable price depends on the size of the pump. Finally, for each added storage, a fixed price of 5000 [€] is used, in order to take into account costs related to the installation of the storage and possible costs related to maintenance. The variable price for the storage is 8 [€/kWh] [20]. The second objective function is the operational cost (OPEX). It is calculated through the aggregation of heat production costs and hydraulic operation (pumping operation, powered by electricity with a given efficiency). Heat costs have a strong temperature dependency related to the technology-specific efficiency dependence on temperature. This is especially the case for Combined Heat and Power (CHP) units, where part of the heat is converted to electricity and the rest is used to heat water. When the targeted temperature for the water is higher, less electricity will be produced, hence a loss of income for the operator of the CHP plant. Then, the cost of heat includes the loss of income associated to electricity production. The cost of the produced electricity is 120 [€/MWh] and the cost of the heat is 50 [€/MWh]. It is important to

note that CAPEX (Capital Expenditure) and OPEX (Operational Expenditure) are considered as independent variables in the decision-making process. This means that they are evaluated separately and comparing them directly is not straightforward, because they represent different aspects of the costs associated with the network modifications. They typically occur at different points in time. CAPEX represents the initial investment required to set up a project or an asset, and it occurs upfront. OPEX, on the other hand, includes the ongoing operating and maintenance costs that are incurred over the entire operational life of the project or asset. Moreover, they serve different financial objectives. CAPEX is primarily concerned with the acquisition or creation of assets and infrastructure necessary for a project, while OPEX deals with the day-to-day operational costs associated with running and maintaining those assets. In order to have comparable values for the CAPEX and the OPEX, the latter is proposed as its net present value over 20 years with a discount rate of 5% [10]:

$$OPEX_{20\ years} = \sum_{y=0}^{20} \frac{OPEX_{1\ year}}{(1 + 0.05)^y}$$

Equation 4

6. Results

The results of the optimization method applied on different test cases are analyzed in this chapter. The results will first be presented in order to validate the new asset (i.e. the storage), added to the multi-asset and multi-objective optimization. Then detailed solutions and behaviors will be explained keeping a global view, at a fixed temperature. Last of all, the impact of the variation of efficiency due to the change of the supply temperature in the network will be detailed.

6.1 Unitary test

In this section, it is proposed a validation and verification methodology for optimization approaches in DH network. This methodology consists in formulating test cases representative of configurations found in the complex DH network yet simple enough to obtain exact or reasonably good solutions. Every configuration is characterized by the possibility to only activate the storages. The verification and validation (V&V) process has been carried out on five test cases:

- Case study 1: only STORAGE_1, positioned at the end of the western branch, is selected in the decision space;
- Case study 2: STORAGE_1 and STORAGE_2 are selected in the decision space;
- Case study 3: the configuration is the same as for case study 2, but here the centralized storage (STORAGE_3) is also considered;
- Case study 4: the configuration is the same as for case study 3 but with STORAGE_4 also considered (the storage is located downstream the pipe of the southern branch with the highest velocity);
- Case study 5: four storages are already considered, this configuration adds the last storage (STORAGE_5), located at the end of the southern branch.

For a clearer comprehension of each scenario's configurations, an image of the network is provided here (Figure 28).

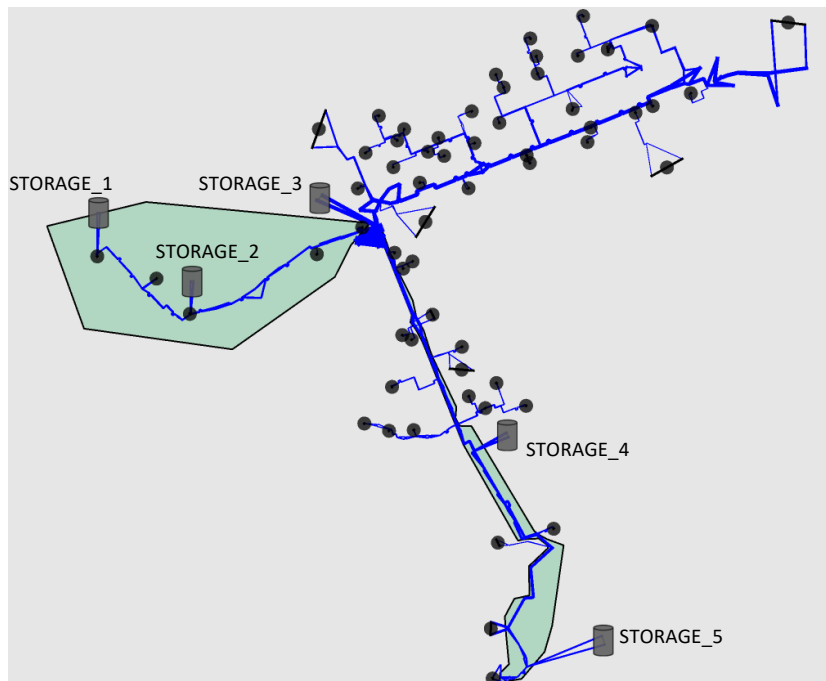


Figure 28. District heating network including five storages.

The aim of this methodology is, not only to verify the modification of the optimization process due to the new asset, but also to evaluate the influence of each storage on the network. In order to do so, a scenario without storage has also been tested. The decision space for the sizes of the storage (presented in the section 5.3.1) are the same for all case studies. Every case study has been tested at four different operational temperatures. For each decision variable, the option to perform no modification on the storage exists, which results in zero investment cost. The results of the unitary test are shown in the Table 5.

Table 5. Validation and Verification Test Scenarios for DH Network Optimization.

T of the supply line	Simulation	5 storages as parameters, adding one storage each scenario				
		CASE STUDY 1	CASE STUDY 2	CASE STUDY 3	CASE STUDY 4	CASE STUDY 5
	NO STORAGE	Storage_1	+ Storage_2	+ Storage_3	+ Storage_4	+ Storage_5
117 [°C]						
116 [°C]						
115 [°C]	Max vel = 2,57 m/s					
114 [°C]	Max vel = 2,76 m/s					

At temperatures 117 [°C] and 116 [°C], every case study satisfies the constraints set in the optimization process. The process shows different results at 115 [°C], this is the temperature at which the subnetwork of Metz presents some criticalities. Here the first three case studies and the scenario without storage are not able to satisfy the constraints, specifically the maximum velocity constraint. Only the addition of STORAGE_4 helps to reduce the velocity in the critical branch. Consequently, also the case study 5 is valid at that temperature. At 114 [°C], none of the case study is valid. Hence, storages are not enough to satisfy the constraints, other assets (pipes diameter, booster pumps and substation size) are needed to be activated.

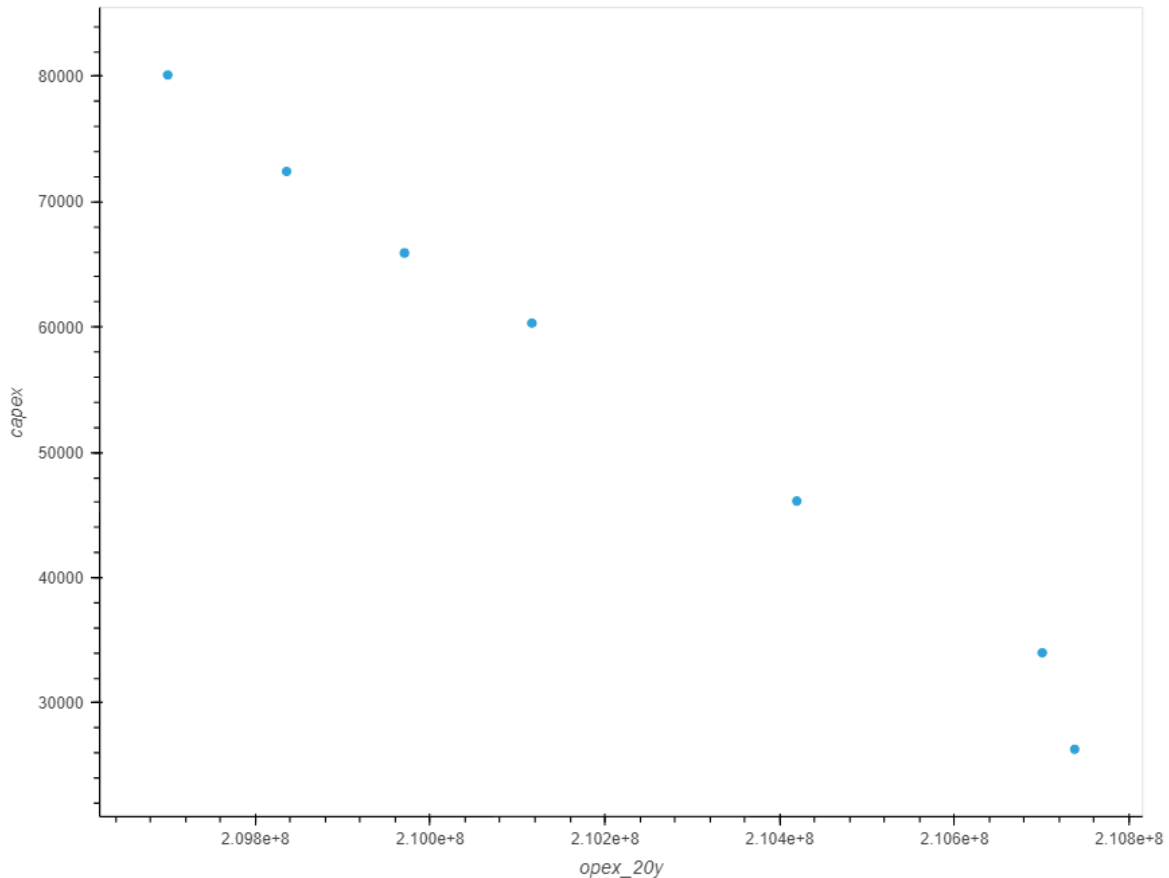


Figure 29. Pareto front of the case study 5 at 115 [°C]

Figure 29 represents the Pareto curve of the case study 5, where each storage could be activated. Every point in the graph represents a different configuration of the network. At higher CAPEX more storages are activated. There is no point at zero CAPEX, given that the operational temperature of the simulation is 115 [°C] and at this temperature the network is not able to satisfy all the constraints.

6.2 Detailed results for a supply temperature of 115 [°C]

The result of an optimization is a set of modifications proposed on the DHN. The scenario presented in this section is characterized by the DHN in which it is possible to perform modifications on the asset of interest (pipes, pumps, substations, storages). When using GA, and specifically NSGA2, some parameters describing the population size, and mutation rate have to be set. The last one is selected thanks to the recommended parameters found in the literature [21], it is a fixed value for every scenario that has been tested; the value is shown in the Table 3 (see section 5.2). The influence of the population size is hard to evaluate, and no generic recommendations have yet been proposed in the field of evolutionary computation. Therefore, the population size is chosen in order to overestimate it, to facilitate the convergence and avoid a lack of diversity in the evolutionary process. The summary of the selected parameters is available in Table 6.

Table 6. Selected parameters for NSGA2 algorithm for the tested case.

PARAMETERS SELECTED FOR NSGA2 ALGORITHM	
Population size	400
Number of generations	200

One set of optimal solutions is presented in Figure 30. It contains the results of the 115 [°C] temperature level. It is essential to provide clarity on the specific components of CAPEX for each scenario:

- Blue curve: scenario with storages;
- Red curve: scenario without storages.

In both scenarios, CAPEX comprises the costs associated with the listed assets, such as added booster pumps, modifications to substation capacities, and adjustments to pipe diameters (defined in section 5.3.2). However, in the scenario with storage, CAPEX also incorporates the costs directly linked to the installation of energy storage solutions. These added expenses represent the initial investments required for the energy storage infrastructure. This distinction clarifies the allocation of CAPEX in both scenarios, enabling a precise understanding of the expenditure considerations. These alterations play a significant role in optimizing the system's efficiency and performance. By distinguishing the distinct CAPEX components for each scenario, the analysis highlights the financial implications of energy storage compared to system improvements, providing a clear understanding of the expenditure allocation in both cases.

The first noticeable result concerns difference in the range of the OPEX objective. The Pareto curve of the scenario with storages is shifted towards the left, it means that the possible configurations of the network, in the scenario that includes the possibility to activate distributed and centralized storages, have lower OPEX due to lower heat losses in the pipe and lower pumping power. Indeed, at the same CAPEX, the scenario with storages gives to the operator the possibility to choose a specific configuration of the network, accounting for lower operational cost.

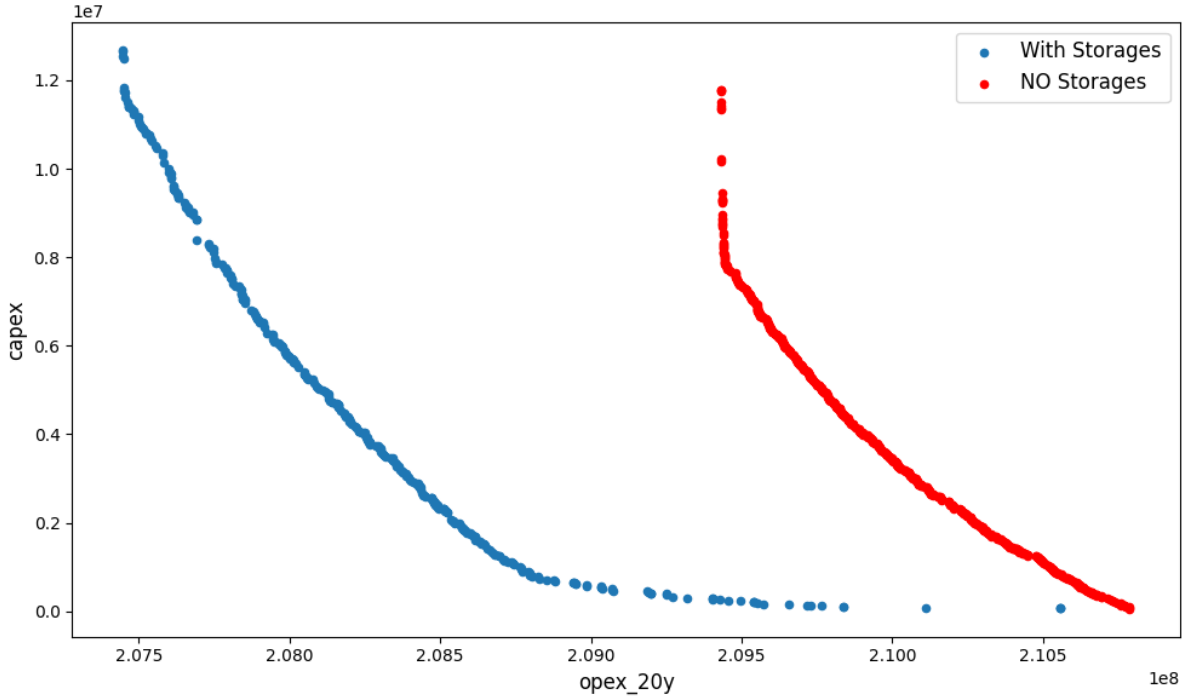


Figure 30. Comparison of the Pareto Curve in two scenarios: with and without storages.

6.2.1 Details on the proposed solution

In order to explore the proposed solution, it is possible to visualize results through a custom view presenting values of some of the decision parameters. Figure 32 pictures changes of volume of the STORAGE_5 (the location is shown in Figure 31). It is noticeable that there is a point that corresponds to the state where OPEX cannot be lowered any further without increasing the storage volume, from 125 [m³] to 196[m³].

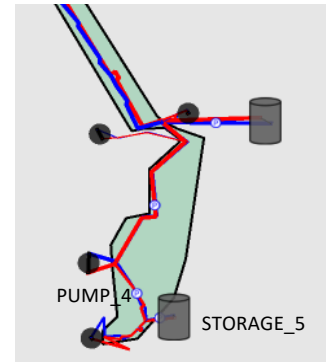
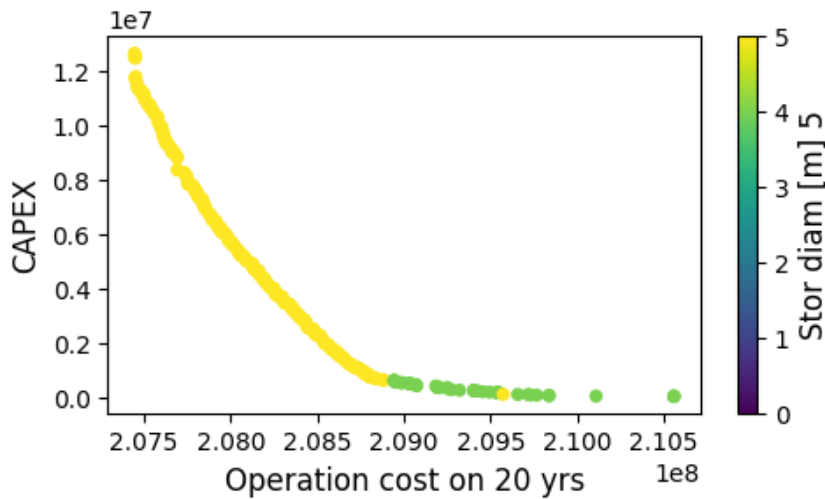


Figure 31. Location of the detailed assets.

Figure 32. Pareto front at 115 [°C] with details on the STORAGE_5.

Thank to this framework feature, it is possible to evaluate some links in between the different assets. Comparing the two graphs in Figure 33 and 34, both describe the behavior of the PUMP_4, on the left the Pareto curve corresponds to the scenario with storages, the right curve corresponds to the scenario without storages. In the latter, the PUMP_4 is almost never activated; in the scenario with storages it is activated, a tipping point is reached and it corresponds with the same tipping point already explored in the case of the STORAGE_5 (see Figure 32).

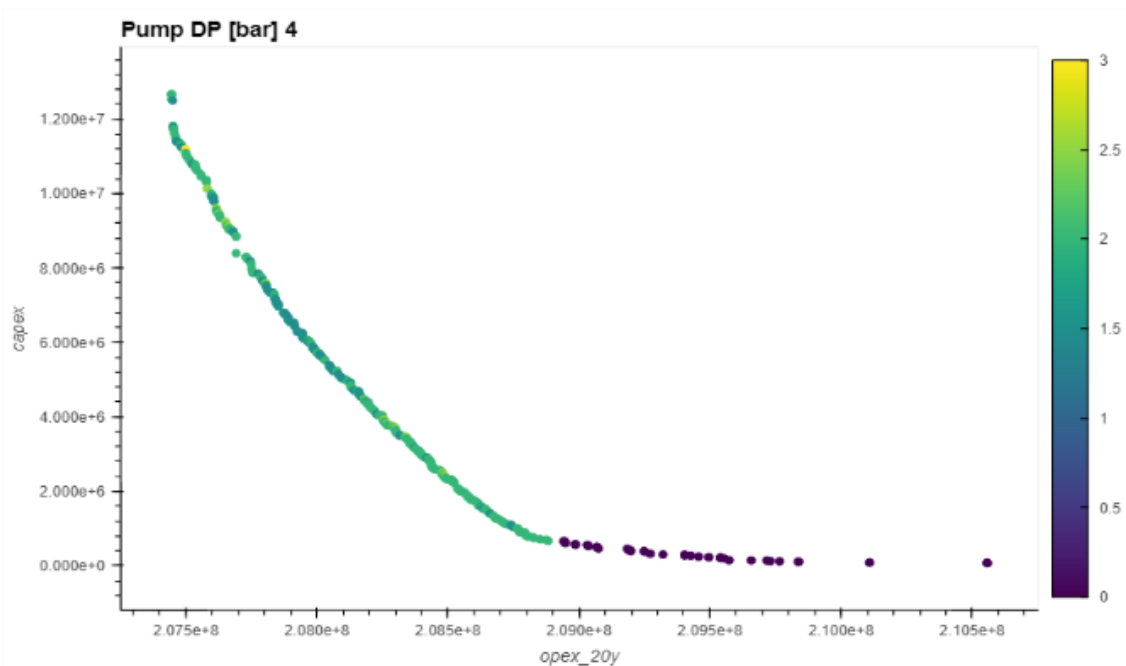


Figure 33. Pareto front at 115 [°C] with details on the PUMP_4 in the scenario with storages.

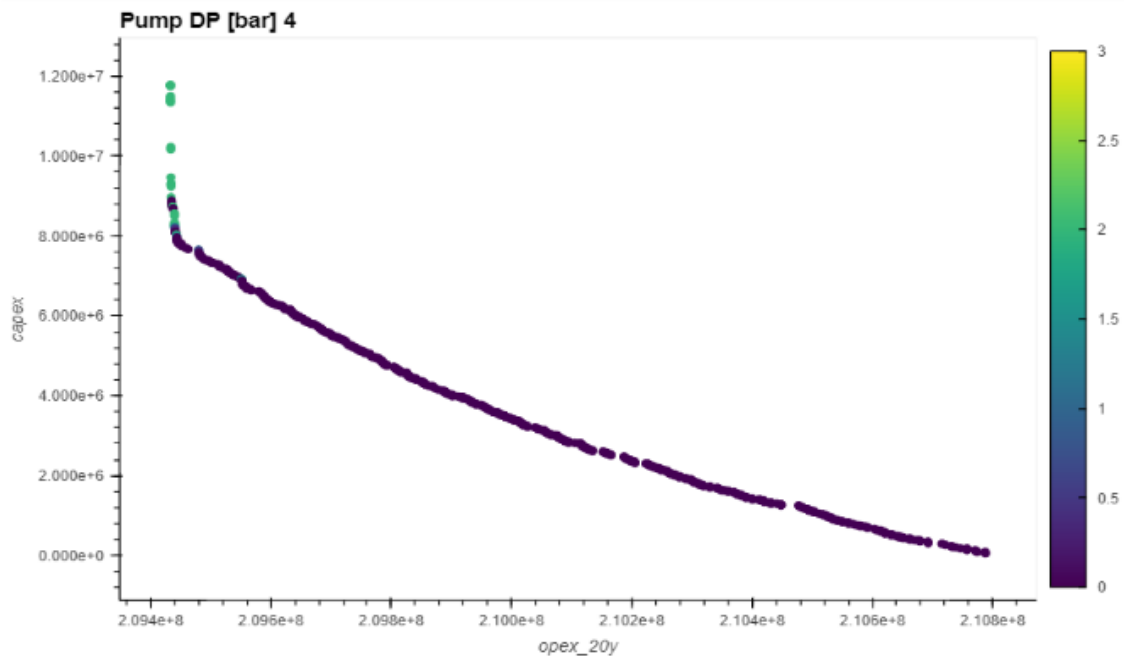


Figure 34. Pareto front at 115 [°C] with details on the PUMP_4 in the scenario without storages.

6.3 Effect of the supply temperature on the results

The same network has been tested at different temperature levels: 115 [°C], 112 [°C], 110 [°C], 109 [°C]. Each scenario has been compared with the scenario without storages. From a global view, all the configurations with storages have lower OPEX with respect the configurations without; at lower temperature the reduction in OPEX is less evident, the gap in between the Pareto curve at 109 [°C] and the one at 110 [°C] is smaller (Figure 35).

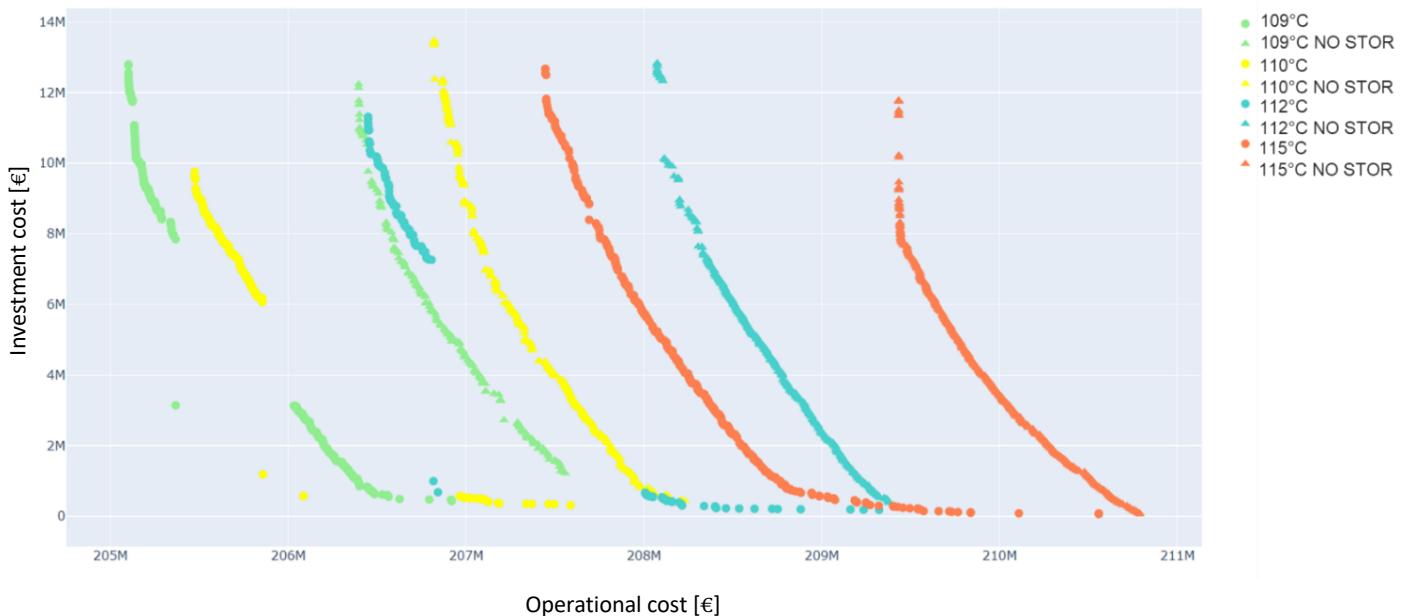


Figure 35. Comparison of the Pareto Curve in two scenarios: with and without storages at four different temperature levels.

The upper figure (35) displays a notable disruption in certain curves (i.e., the curve at 109 [°C] and at 110 [°C]), which can be attributed to the genetic algorithm's inability to achieve convergence at lower

temperatures with the specified number of generations. This observation suggests that the genetic algorithm may need adjustments or additional computational resources to effectively converge at lower temperatures. A potential solution could involve extending the number of generations or optimizing algorithm parameters to improve convergence, especially in scenarios where low temperatures play a critical role.

Also with these different scenarios, it is possible to highlight some linked behavior in between assets. Figure 36 and Figure 37 show, respectively, the behavior of the substation 1 downstream of STORAGE_1 and the behavior of the substation 5 downstream of STORAGE_5, as shown in Figure 38. In both graphs of each figure (Fig.36 and 37), it is possible to evaluate the same trend: when the storage is activated or not, the substation is modified or not, increasing (or not) the sizing power.

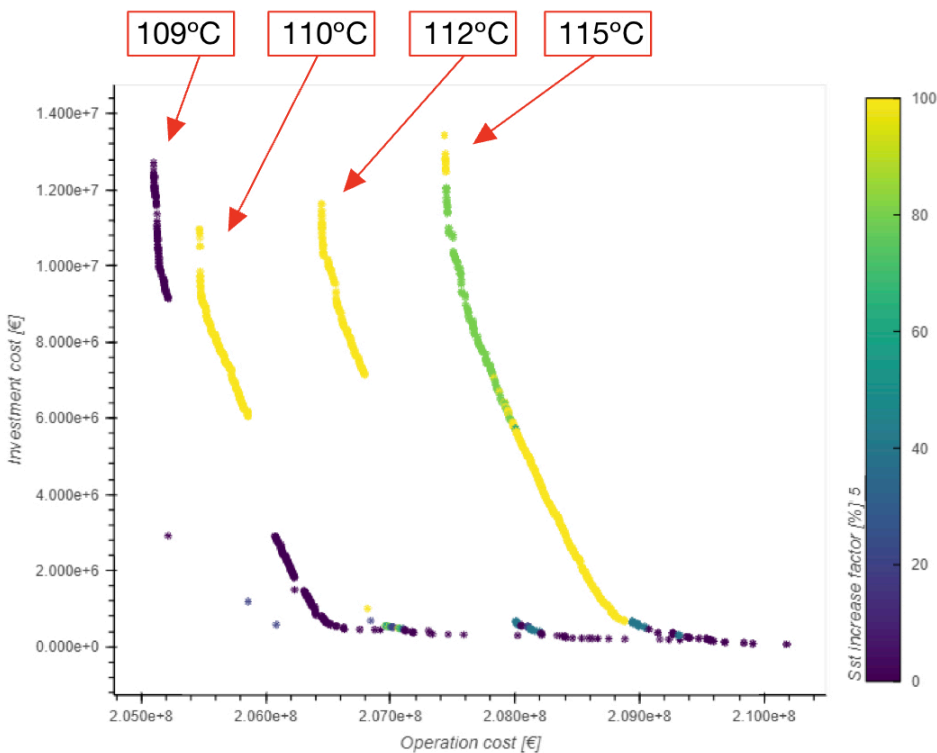
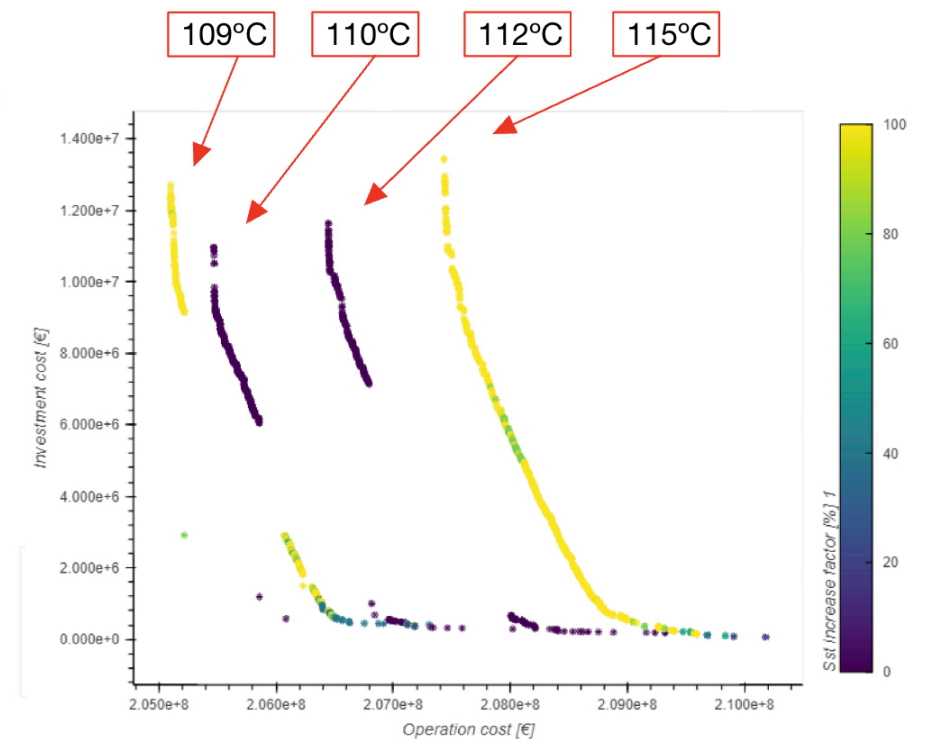


Figure 36. Pareto front at different temperature with details on the SST1 (on the top part) and SST5 (on the bottom part).

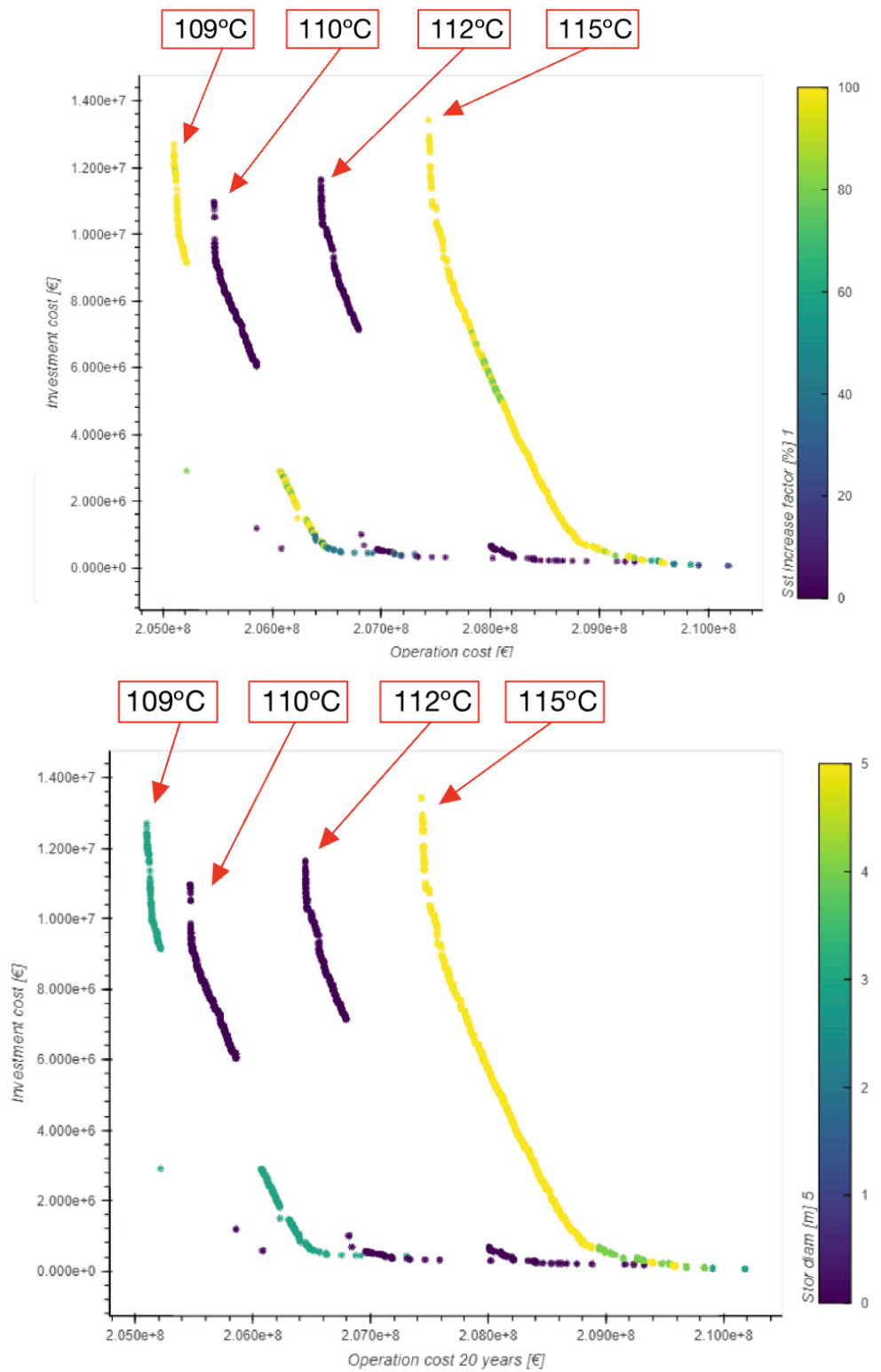


Figure 37. Pareto front at different temperature with details on the STORAGE_1 (on the top part) and STORAGE_5 (on the bottom part).

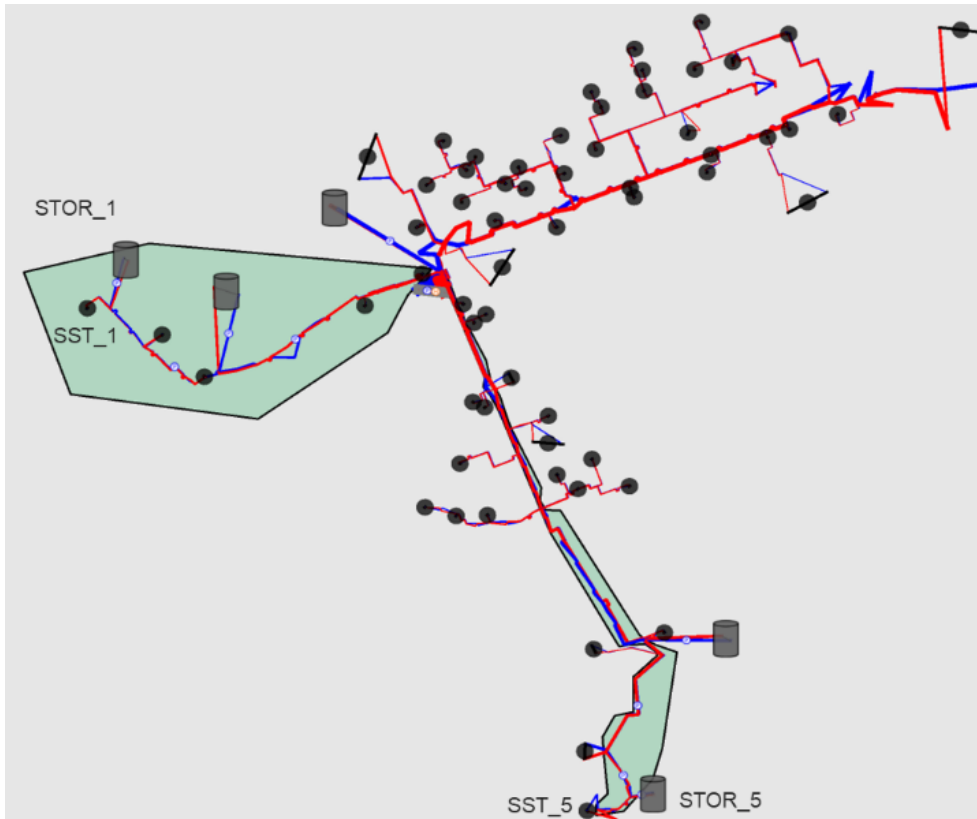


Figure 38. Configuration of the network with the highlighted assets.

6.4 Discussion regarding initial conditions of the storage

The results shown in the previous sections take into account a storage with the following hypothesis of initialization (set by default by the simulator), fixed for each simulation:

Table 7

INITIAL CONDITIONS OF THE STORAGE

Temperature of the hot fluid	100 [°C]
Temperature of the cold fluid	30 [°C]

The temperature distribution of six of the storage layers is pictured in Figure 39.

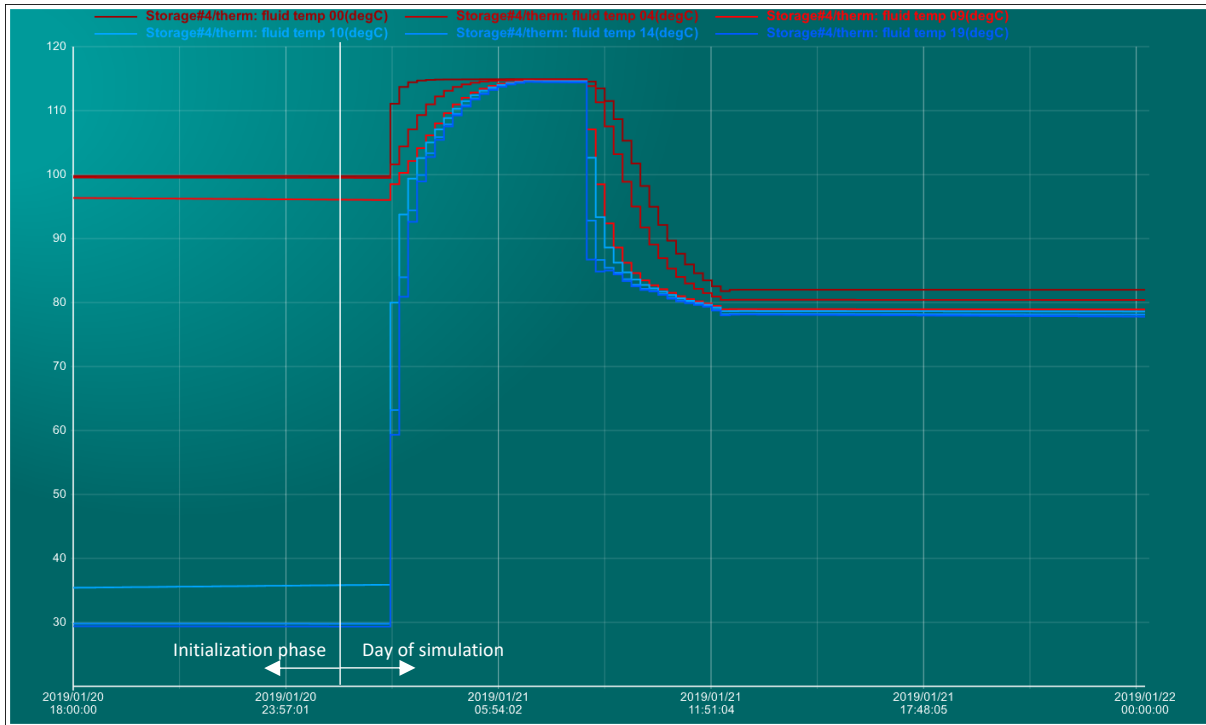


Figure 39. Scenario 1: temperature [°C] distribution inside the storage.

In the real condition of the network, the storage has to be considered empty at the starting time and at the end of each day of simulation. It follows that the initial conditions are modified: the initial condition of the storage has to be the same condition of the end of the discharging time (see Figure 40).

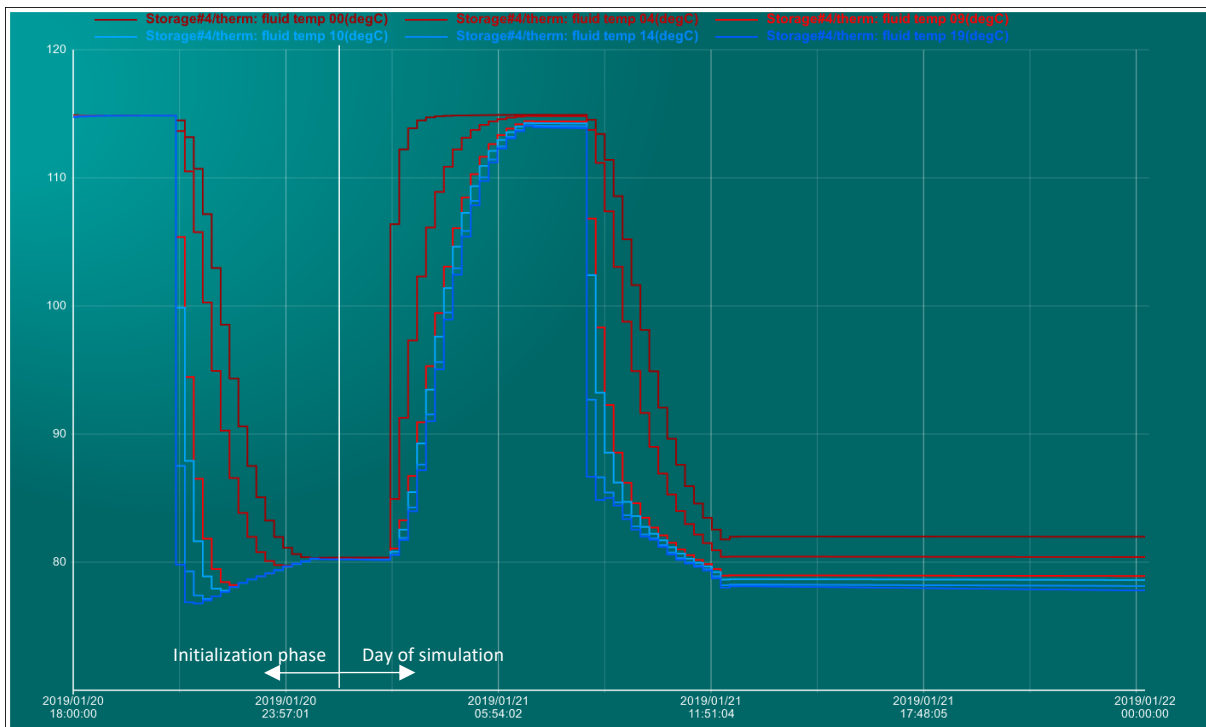


Figure 40. Scenario 2: temperature [°C] distribution inside the storage.

In order to evaluate the effects of the initial conditions of the storage on the network, the two scenarios (1 with the initial condition set by default; 2 with a charging/discharging phase before the simulation day) are analyzed. In both scenarios, only one storage is activated, with the same condition of charging/discharging and with the same volume. As it is possible to evaluate from the figures above, in the scenario 1 all the layers reach the same temperature (≈ 115 [°C]); on the other hand, in the scenario 2, the layers reach different temperatures. This difference is due to the phenomenon of the natural convection; already presented in the section 4.3.3. Globally, the initial conditions affect the request to the central unit in terms of amount of heat, thus, the OPEX calculated in the optimization process. Table 8 shows the cost related to the heating power, to the pumping power and, lastly, the OPEX, calculated in both scenarios. These values are compared with the values for the scenario without storage. The evaluation of the OPEX is performed within the genetic algorithm on a specific day (January 21st), ensuring that the OPEX calculations are aligned with the temporal aspects of the optimization process.

Table 8. Details on the costs for each scenario.

	Scenario 1	Scenario 2	Scenario without storage
Cost for heat injected by the central unit	1832953.16	1833480.24	1833902.65
Cost for energy due to pumping	3947.11341	3964.84325	3898.30135
OPEX	1836900.28	1837445.09	1837800.95

Comparing the scenario 1 and 2, changing the initial conditions, the first one requests less heating power with respect to the scenario 1. It means that the storage, with the initial conditions shown in Figure 39, has a higher amount of energy (before the charging phase) with respect to the scenario 2. Comparing scenario 2 and the scenario without storage, the heating power is higher in the last case and this is due to the fact that at the end of the first phase of charging/discharging the storage is not completely empty. In order to have more precise results, in the context of the optimization, a cyclic simulation is needed in order to assure the same initial and final condition of the storage in the daily scenario.

Due to a lack of time, the new pareto fronts with a better storage initialization (i.e. scenario 2 or even cyclic simulation) could not be calculated.

7. Conclusion and Perspective

In this work a preliminary, but even so meaningful overview concerning how to lower the supply temperature of an already existing District Heating Network through optimal positioning and sizing of Thermal Energy Storages has been provided. In order to study the behavior of distributed storages in the DHN, the realistic case of a subnetwork of the DH Metz network in France has been used for the simulations. A study involving one storage per time has initially been performed in order to evaluate the influence of the presence of a distributed storage in terms of reduction in velocity and in terms of meeting the heat demand. Through this study, the influence of the way in which the storage is charged/discharged has been evaluated, but, due to complexity of the problem, there are still parameters that need to be assessed. The second part of the study concerns the optimization problem. A multi-objective optimization strategy, based on metaheuristics has been used; the aforementioned simulator is used for the solution evaluation. Nonetheless, a systematically-driven number of tests has been carried out trying to add one more storage in the network starting from the results obtained for the $NTES = 1$ case. After using the simulator for identification of relevant assets to be considered as optimization targets, different tests have been carried out with the whole number of parameters that can be modified. The study allowed to extract sets of recommended solutions at a fixed temperature. Lastly, the solution sets are organized as temperature-labeled approximations to Pareto fronts. All solutions are considered as optimal with respect to the fixed economical objectives (OPEX and CAPEX). To summarize, the study reached the following objectives:

- Proof of concept of optimization of distributed storage size and location
- Capacity to find solutions by mobilizing different assets at the same time thanks to a dedicated tool (multi – assets)

While the research has provided valuable insights into the optimization of district heating networks with distributed storages, it is essential to acknowledge certain limitations that have shaped the study. One of the notable limitations encountered during this study pertains to initialization issues in the optimization process. These challenges, particularly in setting initial values for decision variables, can impact the efficiency and convergence of optimization algorithms. Future work should focus on developing robust initialization strategies to mitigate these issues and improve the optimization process's reliability. Despite these limitations, there are promising perspectives for advancing the integration of distributed storages within district heating networks. The integration of distributed storages within the DH network presents exciting opportunities for enhancing network efficiency and resilience. Future perspectives should delve deeper into the technical and operational aspects of integrating distributed storages, as investigating advanced control and management strategies to optimize the usage of distributed storages in real-time, considering factors such as load forecasting, weather conditions, and user demand patterns; exploring emerging technologies, such as advanced materials and energy storage systems, to improve the performance and cost-effectiveness of distributed storage assets; evaluating the environmental benefits of integrating distributed storages, including reduced greenhouse gas emissions and increased utilization of renewable energy sources; conducting economic assessments to determine the cost-effectiveness of distributed storage integration, including factors like payback periods and return on investment.

As regards the optimization tool, in spite of the consistency of these tests, to achieve a more rigorous and reliable result, the control of the storage integration should be refined, adding the possibility to pilot the storage (choosing the storage time, the percentage of charging/discharging). Moreover, in order to highlight the centralized/distributed storage benefits, in terms of decoupling the demand

from the supply in district heating, it is important to integrate the dependency of the OPEX on the power demand. The last point is not considered in this work, the cost reduction due to peak shaving is not accounted. In conclusion, in order to have a clear image of the impact of each asset on the results (Pareto curve), the possibility to read the influence of both pumping power and heating power on the OPEX should be implemented.

This work is not an endpoint but a foundation upon which it will be build a comprehensive Ph.D. project. As progress continues, the aspiration is to refine our understanding of storage control, the role of centralized versus distributed storage, and the dynamic nature of operational expenditures. This research aims to contribute to the evolution of district heating systems toward greater sustainability and efficiency.

Bibliography

- [1] «Section : « Energy system / Buildings / Heating »,» International Energy agency, [Online]. Available: <https://www.iea.org/energy-system/buildings/heating> .
- [2] [Online]. Available: <https://www.iea.org/data-and-statistics/charts/annual-global-energy-supplies-to-district-heating-networks-in-the-net-zero-scenario-2010-2030>. .
- [3] «'DistrictLab | Track 100% of energy losses in thermal grids'.»,» 2022. [Online]. Available: <https://www.districtlab.eu/>.
- [4] [Online]. Available: <http://deap.gel.ulaval.ca/doc/default/index.html>.
- [5] S. W. R. W. S. S. J. E. T. F. H. B. V. M. Henrik Lund, «4th Generation District Heating (4GDH): Integrating smart thermal grids into future sustainable energy systems,» *Elsevier*.
- [6] M. A. N. R. V. E. Guelpa, «Reduction of supply temperature in existing district heating: A review of strategies and implementations,» *Elsevier*, 2023.
- [7] M. C. M. D. M. B. R. F. Simone Buffa, «5th generation district heating and cooling systems: A review of existing cases in Europe,» *Elsevier*.
- [8] C. Delmastro, «Tracking District Heating,» International Energy agency, [Online]. Available: <https://www.iea.org/reports/district-heating>.
- [9] J. W. S. Hongwei Li, «Challenges in Smart Low-Temperature District Heating Development,» *Energy Procedia* , pp. 1472-75, 2014.
- [10] N. R. Y. Merlet, «Optimal retrofit of district heating network to lower temperature levels,» to appear (2023).
- [11] L. P. S. K. T. M. Brange L., «Bottlenecks in district heating networks and how to eliminate them - A simulation and cost study».
- [12] P. Thomsen e P. Overbye, «Energy storage for district energy systems,» in *Advanced district heating and cooling (dhc) systems*, Woodhead Publishing, 2015, p. 339.
- [13] K. M. J. L. J.M. Jebamalai, «Influence of centralized and distributed thermal energy storage on district heating network design,» *Iveiser*, 2020.
- [14] E. G. a. V. Verda, «Thermal energy storage in district heating and cooling,» 2019.
- [15] D. D. Ili', «Classification of Measures for Dealing with District Heating,» 2021.
- [16] M. G. E. E. S. H. Wahiba Yaïci, «Three-dimensional unsteady CFD simulations of a thermal storage tank performance for optimum design,» *Applied Thermal Engineering*, 2013.
- [17] H. JH, «Adaptation in natural and artificial systems,» *University of Michigan Press*, 1975.

- [18] F.-M. D. R. M.-A. G. M. P. a. C. G. F.-A. Fortin, «DEAP: Evolutionary Algorithms Made Easy,» *Journal of Machine Learning Research*, vol. 13, n. 70, p. pp. 2171–2175, 2012.
- [19] R. B. N. V. Yannis Merlet, «Formulation and assessment of multi-objective optimal sizing of district heating network,» *Energy*, 2021.
- [20] F. N. a. A. M. Laura Pompei, «Current, Projected Performance and Costs of Thermal Energy Storage,» *Processes*, 2023.
- [21] R. H. a. Z. M. A' goston Endre Eiben, «Parameter Control in Evolutionary Algorithms,» *IEEE TRANSACTIONS ON EVOLUTIONARY COMPUTATION*, 1999.
- [22] M. G. S. B. M. C. A.M. Jodeiri, «Role of sustainable heat sources in transition towards fourth generation district heating – A review,» *Elsevier*.
- [23] D. W. C. A. E. S. Abdullah Konaka, «Multi-objective optimization using genetic algorithms: A tutorial,» *Elsevier*, 2006.
- [24] «International Energy Agency,» [Online]. Available: <https://www.iea.org/energy-system/buildings/heating>.